Congenital Hyperinsulinism; Effects of Rapamycin on Min6 Pancreatic β-Cell Line

A thesis submitted to the University of Manchester for the degree of Master of Philosophy in the Faculty of Life Sciences

Supervised by:
Dr. Karen Cosgrove

Submitted by:
Osama Basalem

2016

Table of content

List of Figures

Chapter 1

Chapter 2

Chapter 3

List of Tables

Chapter 2

Abstract

Institution: University of Manchester

Name: Osama S. Basalem

Degree title: Master of Philosophy

Date: 2016

Thesis title: Congenital Hyperinsulinism; Effects of Rapamycin on Min6 Pancreatic β-Cell Line.

Introduction: Congenital Hyperinsulinism (CHI) is a rare neonatal syndrome associated with continuous inappropriate insulin secretion by the pancreatic β-cell in the presence of recurring hypoglycemia. Newborn babies with CHI present with hypoglycemia and often do not respond to medical therapy. Although rapamycin has been used to successfully treat a small number of CHI patients, the mechanism of action to reduce insulin secretion is still unclear. The aim of this study was to assess the effects of rapamycin on cell proliferation, apoptosis, insulin secretion and changes in intracellular Ca^{2+} concentration ($[Ca^{2+}]_i$)in Min6 mouse insulinoma β-cell line, an *in vitro* model system that reflects many properties of normal human β-cells.

Methods: Cells were first checked for genetic expression of signaling components required for rapamycin action using RT-PCR. Cell proliferation rate and viability were evaluated by treating the cells with ascending concentrations of rapamycin (0-300 nM) followed by manual cells count using trypan blue dye exclusion during the 4 days of treatment. Cells were checked for apoptotic events via measuring Caspase 3/7 activity following 3 days of treatment with 200 nM rapamycin. Insulin secretion was assessed using ELISA following stimulation with glucose (20 mM), ATP (100 μM), UTP (100 μM), ACh (100 μM) and diazoxide (200 μM) in the presence or absence of short- or longer-term exposure to rapamycin (200 nM). Finally, the effect of rapamycin on $[Ca^{2+}]_i$ was assessed using FlexStation3 after cells were stimulated with ATP+UTP (100 μM each) , ACh (100 μM) and KCl (40 mM) (with and without rapamycin) .

Results: Rapamycin reduced cell proliferation at every concentration used with significant reduction of cell numbers following 4 days of treatment. Treating the cells with rapamycin (200 nM) for 3 days had no detectable caspase activity in Min6 cells. High glucose concentration, ATP, UTP and ACh all elicited robust increases in insulin secretion from Min6 cells. Rapamycin significantly inhibited glucose- and

ATP/UTP/ACh-stimulated insulin secretion back to basal levels. Pre-incubation of Min6 cells in rapamycin prior to insulin secretion experiments resulted in reduced insulin secretion. However, rapamycin did not prevent increases in $[Ca^{2+}]_i$ levels following stimulation with ATP+UTP and ACh.

Conclusion: Rapamycin did not influence changes in intracellular $[Ca^{2+}]_i$ brought about by different stimulators of insulin release. This could mean that rapamycin might be involved in the inhibition of later events in insulin signaling such as recruitment of insulin granules from the reserve pool (Ca^{2+}-dependent), granule movement or docking with the cell membrane. Therefore, further investigations are required to elucidate the mechanism of how rapamycin inhibit insulin secretion.

Declaration

I declare that no portion of the work referred to in the thesis has been submitted in support of an application for another degree or qualification of this or any other university or other institute of learning.

Copyright statement

Acknowledgment

First, I would like to thank my supervisor Dr. Karen Cosgrove for her constant help, guidance and feedback throughout my time at the University of Manchester.

Second, I would like to thank all my laboratory colleagues for their help and support.

I would like to express my deepest appreciation to my parents, my family, my wife, Walaa, my son, Wesam, and all my teachers for making me the man who I am today.

Finally, I would like to thank my sponsor, The Saudi Arabian Cultural Bureau in London, and King Abdulaziz University for funding this project.

Abbreviations

4E-BP1	Eukaryotic translation initiation factor 4E-binding protein 1
ACh	Acetylcholine
ADP	Adenosine diphosphate
ANOVA	Analysis of variance
ATP	Adenosine tri-phosphate
BLAST	Basic local alignment search tool
Bp	Base pair
BrdU	5-Bromo-deoxyuridine
Ca^{2+}	Calcium ion
cAMP	Cyclic adenosine monophosphate
cDNA	Complementary DNA
CHI	Congenital hyperinsulinism
CO_2	Carbon dioxide
DAG	Diacylglycerol
DAPI	4',6-diamidino-2-phenylindole
DEPTOR	DEP domain containing mTOR-interacting protein
Di-CHI	Diffuse hyperinsulinism
DMSO	Dimethyl sulfoxide
DNA-PK	DNA-dependent protein kinase
DNA	Deoxyribonucleic acid
DNase	Deoxyribonuclease
dNTPs	Deoxynucleotide tri-phosphate
EDTA	Ethylene diamine tetra-acetic acid
ELISA	Enzyme-linked immunosorbent assay
ER	Endoplasmic reticulum
FBS	Fetal bovine serum
FITC	Fluorescein isothiocyanate
FKBP12	FK506-binding protein 12
Fo-CHI	Focal hyperinsulinism
gDNA	Genomic DNA
Glut-2	Glucose transporter-2
GSIS	Glucose stimulated insulin secretion

HEPES	4-(2-hydroxyethyl)-1-piperazineethanesulfonic acid
K_{ATP}	ATP sensitive potassium channel
KRH	Krebs Ringer HEPES buffer
M3R	Muscarinic 3 receptor
mLST8	Mammalian lethal with sec-13
mSIN1	Mammalian stress-activated protein kinase interacting protein 1
mTOR	Mammalian target of rapamycin
mTORC1	mTOR complex 1
mTORC2	mTOR complex 2
NGS	Normal goat serum
PBS	Phosphate buffer saline
PDK1	3-phosphoinositide-dependent protein kinase 1PIK
	Phosphatidylinositol kinase
PDX1	Pancreas duodenal homeobox 1
PET	Positron emission tomography
PIP3	Phosphatidylinositol-3,4,5-trisphosphate
PKB	Protein kinase B
PKC	Protein kinase C
PLC	Phospholipase C
PRAS40	Proline-rich AKT substrate 40 kDa
PROTOR	Protein observed with RICTOR
PTEN	Phosphatase and tensin homolog
RAPTOR	Regulatory associated protein of mTOR
RHEB	Ras homolog enriched in brain
RICTOR	RAPTOR independent companion of mTOR
RNA	Ribonucleic Acid
RNase	Ribonuclease
RT-PCR	Reverse transcription polymerase chain reaction
S6K1	Ribosomal protein S6 kinase 1
SEM	Standard error of the mean
SUR1	Sulfonylurea receptor 1
TAE	Tris acetate EDTA
TSC1	Tuberous sclerosis 1

TSC2	Tuberous sclerosis 2
TUNEL	Terminal deoxynucleotidyl transferase dUTP nick end labeling
UTP	Uridine-5'-triphosphate

Chapter 1:

Introduction

1.1 General introduction

Congenital Hyperinsulinism (CHI) is a rare neonatal syndrome associated with inappropriate secretion of insulin by the pancreatic β-cells leading to severe hypoglycaemia and increased pancreatic proliferation rate (Glaser 2000; Dunne et al. 2004; Salisbury et al. 2015). Worldwide, the estimated incidence of CHI is 1:50,000 live births; however, the number can increase in areas where there is genetic consanguinity up to 1:2500 live births (Bellanné-Chantelot et al. 2010; Arnoux et al. 2011).

The most common features of CHI are hyperinsulinaemia and hypoketonaemia, hypofattyacidaemia and hypoglycaemia (Hussain 2007). Due to the hyperinsulinaemic status, the process of gluconeogenesis is reduced and glucose uptake is increased. Therefore, achieving euglycemia is crucial to prevent mental retardation and irreversible brain damage (Menni et al. 2001; De León and Stanley 2007).

There are at least 8 mutations reported in CHI patients. Mutations of K_{ATP} channel subunits sulphonylurea receptor 1 (SUR1) and Kir6.2 genes (*ABCC8* and *KCNJ11*), lead to defective K_{ATP} channel (channelopathy), which are more frequently seen in CHI patients (up to 45% of CHI cases) (Dunne et al., 2004; James et al., 2009). Mutations in the next group of genes lead to metabolopathy in CHI patients and account for less than 10% of CHI cases. Those genes are: *HADH* (encodes 3-hydroxyacyl-coenzyme A dehydrogenase), *GLUD1* (encodes glutamate dehydrogenase), *GCK* (encodes glucokinase), *HNF4A* (encodes hepatocyte nuclear factor 4 α), *SLC16A1* (encodes monocarboxylate transporter 1) and *UCP2* (encodes mitochondrial uncoupling protein 2) (Dunne et al., 2004; González-Barroso et al., 2008; James et al., 2009).

1.2 CHI can be histologically classified into at least two types

CHI is classified into two forms: Diffuse Hyperinsulinism (Di-CHI) and Focal Hyperinsulinism (Fo-CHI). In the diffuse form, the entire pancreas is affected, whereas in the focal form, the disease is limited to a small area of the pancreas (usually 2.5 mm to 7.5 mm in diameter) (Arnoux et al., 2011). Therefore, the focal form may be treated surgically by removing affected areas. Furthermore, different studies reported that around 50% of CHI cases are those with focal form (de Lonlay-Debeney et al., 1999; Glaser, 2000; Dunne et al., 2004; De León and Stanley, 2007).

Fo-CHI arises from a combination of paternally inherited mutations of K_{ATP} channel genes (*ABCC8* or *KCNJ11*) along with somatic maternal haploinsufficiency (De Lonlay et al., 1997; Arnoux et al., 2011), whereas Di-CHI is predominantly due to autosomal recessive inheritance of K_{ATP} channel gene mutations (*ABCC8* or *KCNJ11*) (Dunne et al., 2004; Arnoux et al., 2011).

1.3 Pathophysiology of CHI and Glucose Stimulated Insulin Secretion (GSIS)

β-cells respond to increase in blood sugar by secreting insulin by a mechanism known as Glucose Stimulated Insulin Secretion (GSIS). Glucose enters the β-cells via glucose transporter-2 (glut-2) and is metabolized by glucokinase (hexokinase IV) first to form glucose-6-phosphate, which enters a series of reactions (glycolysis, citric acid cycle and electron transport chain) (Lenzen, 2014). Sugars, as well as other nutrients such as fatty acids catabolism, lead to an increase of intracellular concentrations of ATP relative to ADP. The difference in ATP/ADP ratio within the β-cell causes the ATP-sensitive potassium channels (K_{ATP}) to close. This closure causes buildup of positively charged K^+ ions within the β-cell and the membrane potential becomes more positive, initiating cell membrane depolarization. The depolarization then leads to the opening of the voltage-sensitive calcium channels causing Ca^{2+} influx. As Ca^{2+} enters the cell, it triggers the release of insulin molecules by exocytosis (Dunne et al., 2004). Figure 1.1 summarizes the process of GSIS in β-cells.

The K_{ATP} channel is a functional octamer of 4 selective pore-forming subunits Kir6.2 (creating the central pore) linked to 4 outer SUR1 regulatory subunits (Enkvetchakul and Nichols, 2003). SUR1 is an ATP binding cassette protein and receptor for sulfonylureas, whereas Kir6.2 is an inward rectifier K^+ channel (Dunne et al., 2004; Vedovato et al., 2015). The activity of K_{ATP} channel can be modulated via the Kir6.2 and SUR1 subunits (Vedovato et al., 2015). Interaction with Kir6.2 subunits with phosphoinositide lipids can activate the K_{ATP} channel, while ATP inhibits the channel activity. On the other hand, K^+ channel opener drugs (like diazoxide) and MgATP act on SUR1 subunits to activate the K_{ATP} channel, while sulfonylureas inhibit the channel activity (Enkvetchakul and Nichols, 2003; Dunne et al., 2004; Vedovato et al., 2015).

As mentioned above, the most common mutations that cause CHI are those affecting the K_{ATP} channel functional subunits SUR1 or Kir6.2, which are encoded by *ABCC8* and *KCNJ11* genes respectively (Nestorowicz et al., 1996; Thomas et al., 1996; Glaser, 2000; De León and Stanley, 2007; Hussain, 2007). Understanding the K_{ATP} channel role in the mechanism of GSIS and finding a mechanism to interfere with the inappropriate insulin release could help researchers design new treatments for CHI.

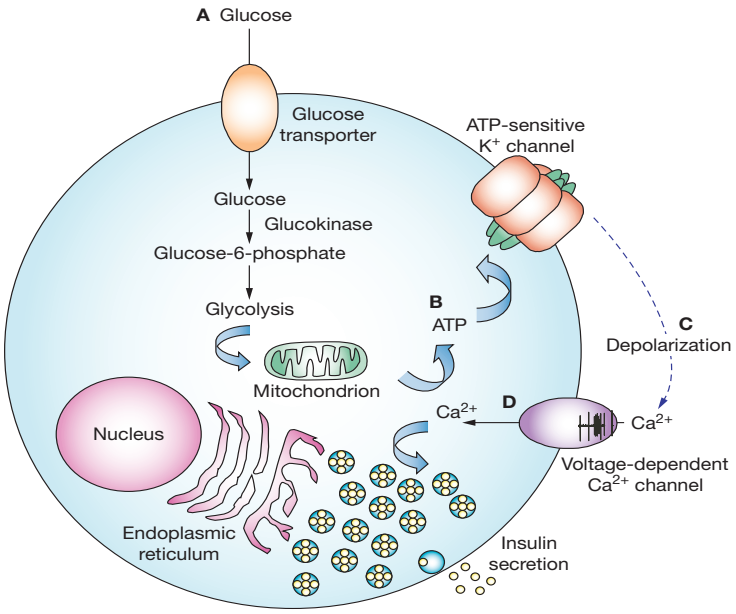

Figure 1.1: Mechanism of Glucose Stimulated Insulin Secretion (GSIS) in β-cells. Glucose is transported into the β-cell via glucose transporter-2. Then, metabolism is initiated by glucokinase. **B**. As the glucose is metabolized, the ratio of ATP:ADP is increased, causing the closure of K_{ATP} channel. **C**. The previous event causes the β-cell membrane to be depolarized. This results in opening of the voltage dependent Ca^{2+} channel. **D**. Ca^{2+} influx results in insulin secretion via exocytosis (De León and Stanley, 2007).

In addition to GSIS, insulin release can be stimulated via several receptors on the β-cell membrane. One of those receptors is the muscarinic acetylcholine receptor (M3R), which is a member of the G protein family (Bordin et al., 1995; Boschero et al., 1995). Once the neurotransmitter agent acetylcholine (ACh) binds to the receptor, it causes the activation of the M3R. The principal behind the induced insulin release is as follows:

Upon activation of the M3R, hydrolysis of the membrane phospholipid via phospholipase (PLC) beta causes the production of Diacylglycerol (DAG) and inositol 1,4,5-trisphosphate (IP_3) (Bordin et al. 1995). DAG is involved in the activation of several forms of protein kinase C (PKC), while IP_3 is involved in intracellular Ca^{2+} release from intracellular stores. The combined effect of IP_3 binding to its specific receptor, and PKC activation results in more Ca^{2+} being released, hence insulin release is maximized (Bordin et al. 1995; Boschero et al. 1995).

Extracellular ATP release by the pancreatic acinar cells, exocrine pancreas, or from the nerve endings supplying the pancreas (Burnstock and Novak, 2013) has a stimulating effect on insulin secretion from mouse islets (Petit et al., 1989). The β-cell has two types of purinergic receptors, P2X and P2Y (Khan et al., 2014), through which extracellular ATP and UTP can bind and modulate insulin release. P2X is an extracellular ATP-gated cation channel while P2Y is an ATP-sensing G-protein coupled receptor (Schwiebert and Zsembery 2003; Schwiebert et al. 2005; Richards-Williams et al. 2008; Khan et al. 2014). P2X receptors are Ca^{2+} permeable and can be modulated by extracellular Ca^{2+} leading to Ca^{2+} influx, while P2Y receptors increase free Ca^{2+} concentration from internal stores via phospholipases (mainly phospholipases Cβ) (Schwiebert and Zsembery, 2003). ATP can recognize and bind strongly to P2X and activate the receptor, while UTP binds with low affinity to the P2X receptor (Hattori and Gouaux, 2012). On the other hand, ATP and UTP equally activate P2Y(Burnstock, 1997).

There are different subtypes of both receptors, which raises several arguments regarding which subtypes are involved in insulin secretion *in vivo* (Wuttke et al., 2013; Khan et al., 2014). However, more studies are revealing that the binding of the exogenous ATP to the specific receptor $P2Y_1$ will stimulate insulin secretion (Poulsen et al., 1999; Wuttke et al., 2013; Khan et al., 2014).

Khan et al. (2014) demonstrated that extracellular ATP sends positive autocrine signals to the β-cells to stimulate insulin release via activating $P2Y_1$ receptor. The group investigated whether ADP would have the same effect as ATP on P2Y receptors, and found that ADP and the P2Y receptor agonist MRS-2365 showed the same effect as ATP. The activation of the receptor has a pivotal part in the regulation

of electrical activity of Ca^{2+} and insulin secretion in human β-cells, which eventually will augment the release of insulin (Khan et al. 2014).

1.4 Management and treatment of CHI

Persistent hypoglycemia in CHI is the most challenging task to manage, with a general treatment aim of keeping the blood glucose level above the lower limit of 3.5 mmol/L (Güemes et al. 2015). Glucose infusion as well as continuous feeding is important to achieve euglycemia. Glucagon may be used if the blood glucose level is severely low in an attempt to stimulate gluconeogenesis and glycogenolysis. Two drugs are currently used in treatment of CHI: diazoxide and octreotide (Dunne et al., 2004). Diazoxide has a direct effect on the K_{ATP} channels of the β-cell. The drug action is to open the K_{ATP} channels in order to cause membrane hyperpolarization, which ultimately reduce the activity of voltage-dependent Ca^{2+} channel (Dunne et al., 2004).

However, not all CHI cases respond effectively to diazoxide, as it requires that a functional subunit should be present on the surface of the β-cell (De León and Stanley 2007). Furthermore, because the drug is antidiuretic in nature, most patients have sodium and fluid retention as a side effect of the drug (Arnoux et al., 2011). Therefore, a diuretic drug, such as chlorothiazide, is often used in combination with diazoxide (Dunne et al., 2004).

Octreotide binds with high affinity to somatostatin receptor 2 and 5, moderate affinity to somatostatin receptor 3 and little or no affinity for somatostatin receptor 1 (Doyle and Egan, 2003). Although β-cells express somatostatin receptor 1 and 5, other tissues express the same receptors as well as other types of somatostatin receptors such as the brain and the gastrointestinal tract (somatostatin receptor 1-5), the adrenal gland (somatostatin receptor 2), the liver (somatostatin receptor 3) and the heart (somatostatin receptor 4) (Bronstein-Sitton, 2006). Therefore, octreotide will not only supress insulin secretion, but also other hormones from the mentioned organs (Doyle and Egan, 2003).

Nevertheless, diarrhoea, abdominal discomfort and cholelithiasis have been reported as a side effect of octreotide (Dunne et al., 2004).

1.4.1 Surgery

When the patient is non-responsive to treatments, surgical intervention is necessary to restore euglycaemic status. The focal form can be defined as local hyperplasia of endocrine cells (including β-cells) (Senniappan et al., 2013). On the other hand, hyperactivity as well as hypertrophy and hyperplasia of β-cells has been observed in the diffuse form of CHI (Sempoux et al. 2004; Senniappan, et al. 2013; 2016). The two forms can be distinguished from each other preoperatively by imaging techniques such as Fluorine-18-L-dihydroxyphenylalanine positron emission tomography (^{18}F-DOPA PET/CT) and pancreas histology (Dunne et al. 2004; Chandran et al. 2013; Yen et al. 2016). After classifying the type of hyperinsulinemia the surgery team can perform the surgery accordingly.

In addition, the histology of different parts of the pancreas (head, the isthmus, the body and the tail) would support the PET result and guide the surgeon to localize the focal form and excise it. In contrast, patients with diffuse form who do not respond to medical therapy will need to undergo near total pancreatectomy (Yen et al. 2016; Senniappan, et al. 2013).

1.4.2 Rapamycin as a new treatment for CHI

Rapamycin is an immunosuppressive drug that is used following transplant of organs and islets of Langerhans to treat type-1 diabetes (Bruni et al. 2014). The drug is also known to have an antiproliferative effect on β-cells, as well as other cell types (Zahr et al. 2008).

Rapamycin has a direct target denoted as the mammalian target of rapamycin (mTOR). Recently rapamycin has been used to treat a small number of patients with severe diffuse CHI, thus avoiding surgery (Shah et al. 2015; Senniappan et al. 2016). Shah et al. (2015) showed a complicated case of CHI patient who was not responding to diazoxide and treated with rapamycin. Rapamycin treatment helped improve glucose homeostasis to the point where glucose and glucagon infusion was no longer required. The reduction in β-cell proliferation and insulin secretion by rapamycin was sufficient to maintain euglycaemia in the patient (Shah et al. 2015). However, the exact mechanism for reducing the insulin secretion is not fully understood.

Treatment with rapamycin exposes newborns to unpleasant side effects such as stomatitis, increased risk of infection, immunosuppression, renal malfunction, fatigue, mucositis and pneumonitis (Sankhala et al. 2009; Senniappan et al. 2014; 2016). Therefore it must be used with caution.

1.5 mTOR complexes and subunits

The mTOR pathway participates in pivotal cell mechanisms and processes such as cell growth, proliferation metabolism and survival (Watanabe et al., 2011). mTOR has two complexes: mammalian target of rapamycin complex1 (mTORC1) and mammalian target of rapamycin complex2 (mTORC2). Each complex has unique subunits, functions and effects on β-cell function (Watanabe et al., 2011).

mTORC1 shares the following subunit composition with mTORC2: mTOR, mammalian lethal with SEC13 protein 8 (mLST8) and domain–containing mTOR-interacting protein (DEPTOR) (Barlow et al., 2013; Pópulo et al., 2012; Peterson et al., 2009; Hara et al., 2002). However, mTORC1 also has unique proteins such as regulatory associated protein of mTOR (RAPTOR), proline-rich Akt substrate of 40 kDa PRAS40 and DEPTOR. RAPTOR functions as the scaffolding protein for mTORC1 substrates (Hara et al., 2002; Peterson et al., 2009; Pópulo et al., 2012; Barlow et al., 2013).

mTORC2 also contains proteins which are not expressed in the mTORC1 complex such as rapamycin-insensitive companion of mTOR (RICTOR), in addition to mTOR, mLST8, Protor and DEPTOR (Hara et al., 2002; Peterson et al., 2009; Pópulo et al., 2012; Barlow et al., 2013). Figure 1.2 shows the components of mTORC1 and mTORC2 (Pópulo et al. 2012).

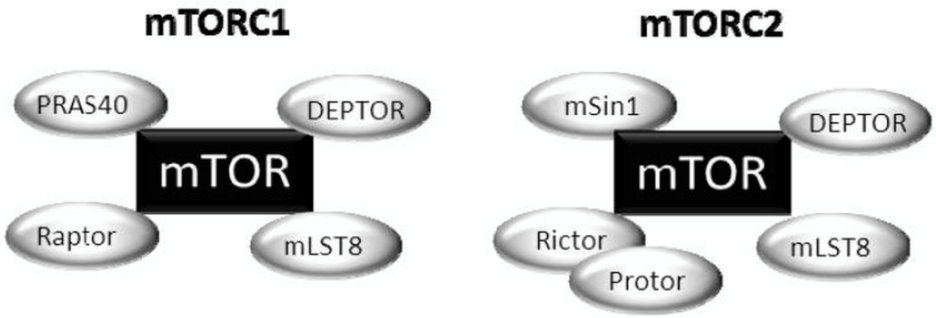

Figure 1.2: shows the composition of mammalian target of rapamycin (mTOR) complexes. mTORC1 is composed of mLST8, mTOR, DEPTOR, RAPTOR and PRAS40. mTORC2 has mLST8, mTOR, mSin1, Protor, DEPTOR and RICTOR (Pópulo et al. 2012).

Interestingly, accumulating data suggests that mTORC1 is rapamycin sensitive, while mTORC2 is relatively rapamycin resistant. However, mTORC2 can show rapamycin sensitivity if treatment is prolonged (Zeng et al. 2007; Barlow et al. 2012; 2013). Furthermore, multiple studies on different cell lines (including the mouse pancreatic β-cell line Min6) show that when mTORC2 is treated with rapamycin overnight, the cells lose the resistance to the drug and become susceptible to rapamycin treatment (Zeng et al. 2007; Barlow et al. 2012; 2013).

1.6 Mechanism of action of rapamycin

First, when rapamycin enters the cell, it binds to FKBP12 (FK506-binding protein of 12 kDa), an intracellular immunophilin protein, to form a complex (Shimobayashi and Hall 2014). Then, this complex interacts with the rapamycin-binding domain (FRB) of mTOR and inhibits mTORC1 functions (Laplante and Sabatini 2009; Shimobayashi and Hall 2014). Since the mTOR pathway is involved in protein synthesis, glucose metabolism and many more essential cell functions which impact on cell survival, inhibition of mTOR leads to cell cycle arrest and reduced cell proliferation (Sehgal 2003; Pópulo et al. 2012; Shimobayashi and Hall 2014).

1.6.1 Phosphoinositide 3'-kinase-Akt (PI3K/Akt/mTOR) signaling pathway

mTOR is capable of functioning downstream of the PI3K/Akt signaling pathway. Generally, once the appropriate growth factor is bound to the extracellular domain of its corresponding receptor tyrosine kinase (such as insulin-like growth factor-1 receptor) on β-cell, it induces receptor dimerization, auto-phosphorylation of the receptor and phosphorylation of intracellular substrates docking sites such as insulin-like receptor substrates). These events trigger the activation of the serine/threonine kinase PI3K pathway (Rothenberg et al. 1995; Sekulić et al. 2000; Chitnis et al., 2008; Hemmings and Restuccia 2012; Stewart et al. 2015). Upon activation, phosphatidylinositol (3,4,5)-trisphosphate (PIP3) is generated at the plasma membrane, at which the Akt interact with PIP3. This interaction partially activates Akt via the phosphorylation of the activation loop at Thr308 of Akt by 3-phosphoinositide-dependent protein kinase 1 (PDK1) (Hemmings and Restuccia 2012). The partially activated Akt can activate mTORC1 by the phosphorylation and inactivation of PRAS40 and tuberous sclerosis protein 2 (TSC2). Then protein synthesis and cell proliferation is up regulated due to the phosphorylation of

ribosomal machinery protein (S6K1). This event activates protein synthesis as the eukaryotic translation initiation factor 4E binding protein 1 (4E-BP1) and S6K1 are substrates of mTORC1 (Sekulić et al. 2000; Hemmings and Restuccia 2012).

Fully activated Akt can be achieved via either mTOR or DNA-dependent protein kinase (DNA-PK), a member of PIK family (subfamily of PI3K) (Priestley et al. 1998), by the phosphorylation of Akt at Ser473 in the C-terminal end motif (Hemmings and Restuccia 2012). The fully activated enzyme mediates many cell functions such as protein synthesis and proliferation, as it is integrated in many signaling pathways (Sekulić et al., 2000; Hemmings and Restuccia, 2012). Dephosphorylating Thr308 the activation loop, Ser473 and PIP3 via PP2A, PHLPP1/2 and PTEN respectively will inhibit the PI3K-Akt pathway (Sekulić et al., 2000; Hemmings and Restuccia, 2012). Figure 1.3 summarizes the signaling pathway of PI3K/Akt/mTOR (Huang et al. 2014; Jóźwiak et al. 2014).

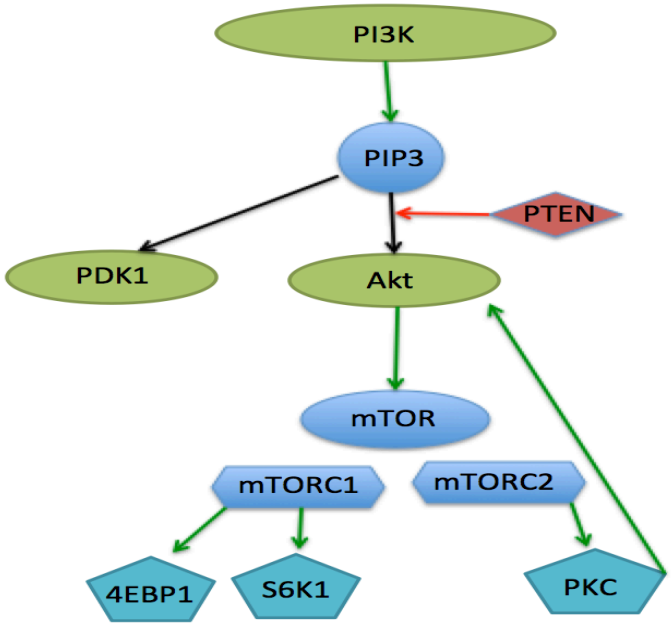

Figure 1.3: PI3K/Akt/mTOR signaling pathway in β-cell. PI3K phosphorylates and activates PIP3, which then binds to PDK1 and Akt. PDK1 and Akt are recruited at the cell membrane, where Akt phosphorylates and activates mTOR. mTORC1 activates 4EBP1 and S6K1, while mTORC2 activates PKC. (Arrows in green, activates; black, binds to; red, inhibits (Huang et al. 2014; Jóźwiak et al. 2014).

One of the proteins downstream to the PI3K signaling pathway is $p70^{S6K}$ (Sekulić et

al., 2000). This protein holds the "key" for progression of the cell cycle and most importantly protein synthesis (Jefferies et al. 1994; Sekulić et al. 2000). Upon treatment with rapamycin, $p70^{S6K}$ is dephosphorylated and inactivated. It is still uncertain how this is done (Graves et al., 1995; Beretta et al., 1996; Sekulić et al., 2000; Peterson et al., 2009).

In summary, treatment with rapamycin for 60 minutes is sufficient to reduce insulin secretion when the number of cells is similar (Fuhrer et al., 2001). Although some information is available on how rapamycin affects cell proliferation, it is unclear how these pathways interfere with insulin secretion, or indeed whether rapamycin exerts effects on insulin secretion via other pathways. Considering that rapamycin has been used successfully to treat CHI in a small number of patients already, it would be beneficial to understand its mechanism of action on β-cells more thoroughly, so that in future more specific drugs can be designed, with fewer side effects.

1.7 Project aims

The aim of the current study was to assess the effects of rapamycin in Min6 cells (a mouse insulinoma cell line capable of GSIS) on cell proliferation and insulin secretion stimulated via different pathways in order to further understand how rapamycin may be effective as a treatment for CHI.
Specific objectives were as follows:

[1] To construct growth curves for the effects of ascending concentrations of rapamycin on cell proliferation rate in Min6 cells utilizing manual cell counts.

[2] To assess cell death in Min6 cells after treatment with rapamycin using trypan blue dye exclusion (for apoptosis and necrosis) and caspase activity (for apoptosis).

[3] To assess insulin secretion from Min6 cells in response to glucose, ATP, ACh and UTP using ELISA.

[4] To assess the effects of rapamycin on GSIS and insulin secretion stimulated by other mechanisms (ATP, ACh and UTP) in Min6 cells.

[5] To assess changes in intracellular Ca^{2+} from Min6 in response to glucose, ATP + UTP, ACh and KCl with rapamycin treatment.

Chapter 2: Materials and Methods

2.1 Cell culture

Mouse insulinoma cell line (Min6) was used in this project (passage 18-33) (Miyazaki et al., 1990; Ishihara et al., 1993). To set up a flask of Min6 cells for experiments, a new vial of Min6 was taken from liquid N_2 reservoir and thawed. Then, 6 ml of pre-warmed culture medium was added to the defrosted cells. Next, the mixture was centrifuge at 47 g in BOECO U-32 centrifuge (Hamburg, Germany) for 5 minutes. Then, the pellet was resuspended in 2 ml of culture media and mixed thoroughly. The cell suspension was inoculated into sterile T25 flasks (Corning Incorporated, New York, USA) and diluted with medium. The culture medium was changed every 48 hours.

Min6 cells were maintained in Dulbecco's modified Eagle medium (DMEM; 4500 mg/L glucose, + L-glutamine, + pyruvate; Gibco, Paisley, UK) supplemented with 15% heat-inactivated foetal bovine serum (FBS) (Gibco, Life Technology, Paisley, UK), penicillin/streptomycin (100 units/ml, 100 µg/ml), 100 µg/ml L-glutamine, and 5 µl/L beta-mercaptoethanol in T25 cell culture flasks. Cells were incubated at 37°C in a humidified incubator supplemented with 5% CO_2. The culture medium was changed every 48 hours. Cells were not allowed to reach more than 60-70% confluence and were subsequently passaged at appropriate ratios. On average the cells were passaged once or twice per week. Trypsin-EDTA (Sigma, Dorset, UK) was the method used in detaching cells from the flask.

2.1.1 Passage of Min6 cells

Cells were allowed to grow until 50-60% confluency was reached. Existing culture medium was removed. Each flask was washed twice with 6 ml of pre-warmed phosphate-buffered saline (PBS) (Sigma, Dorset, UK) followed by 1 ml of pre-warmed trypsin and incubated for 3-5 minutes at 37°C in a humidified incubator supplemented with 5% CO_2. After confirming cell detachment under the microscope, 4 ml of fresh medium was added to inactivate the action of trypsin. The mixture was mixed well and centrifuged for 5 minutes at 47 g in BOECO U-32 centrifuge at room temperature. Next, the supernatant was carefully removed, without disturbing the pellet, and the pellet was resuspended in 2 ml of medium. The cell suspension was mixed thoroughly by pipetting the mixture up and down before transferring 1 ml of

cell suspension into a sterile T25 flask. The transferred amount was diluted with either 5 ml or 6 ml of culture medium. Flasks were incubated overnight at 37°C in a humidified incubator supplemented with 5% CO_2 until cells reached 50-60% of confluency. The culture medium was changed every 48 hours. The ratio of 1:5 was routinely used throughout the project (1 ml of cell suspension + 4 ml of medium). However, 1:6 and 1:4 ratios were used as backup flasks to be either frozen or passaged for future experiments. With 1:5 ratio, cells were approximately splitted once a week to reach 50% confluency.

2.1.2 Freezing cells for long-term storage

Once the cells reached 50-60% confluency, they can be frozen for future work. Cells were treated as if they were to be split following the steps mentioned above. However, cells were resuspended in 200 µl medium, instead of 2 ml, to be transferred to a cryovial. Next, freezing mixture was prepared as: 450 µl medium+ 450 µl FBS + 100 µl dimethyl sulfoxide (DMSO) (Sigma, Dorset, UK). Then, 800 µl of the freezing mixture was added to the vial containing the cell suspension. The vial was then placed in a freezing container (with a 1°C/min cooling rate) to be placed in -80^0 C freezer overnight. The cryovial was transferred the next day to liquid N_2 container to be stored.

2.1.3 Cell count using haemocytometer

Once the pellet was resuspended in medium, 1:1 ratio of cells was mixed with trypan blue (Sigma, Dorset, UK). After mixing the trypan blue cell suspension thoroughly, 10 µl of the suspension was transferred into a clean haemocytometer for counting. The haemocytometer consisted of 9 primary squares and each square was subdivided into 16 secondary 4x4 squares Fig. 2.1. In order to count the cells, cells in the outer squares (i.e. A, C, G and I) were counted. The average cell count was obtained and multiplied by the dilution factor and 10^4 to get the total number of cells per ml (WHO, 1999).

In summary: total number of cells counted in 4 squares ÷ 4 X dilution factor X 10^4.

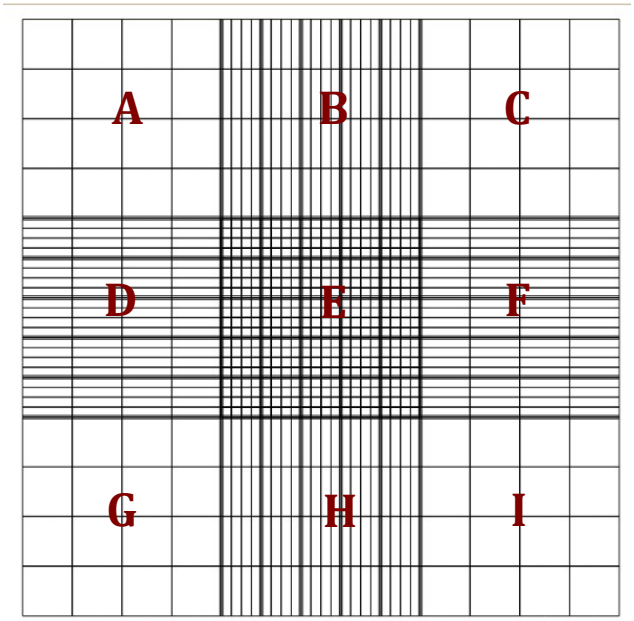

Figure 2.1: haemocytometer gridlines. Every primary square consists of 16 secondary 4x4 squares. Each primary square measures 1mm x 1mm (WHO, 1999).

2.2 Effects of rapamycin on growth curve in Min6 cells

Cells were trypsinized and counted as in Section 2.1.1 and 2.1.3 to be plated in a 24-well plate at the density of 50,000 cells/well in 1 ml of medium. The culture medium was changed every 48 hours. The mTOR inhibitor, rapamycin (Stratech Scientific Ltd, UK), was used at the following concentrations: 300 nM, 200 nM, 100 nM, 10 nM and control.

Three wells were counted daily and an average of these was taken for 4 consecutive days to produce a growth curve using Microsoft Excel.

2.3 Assessment of cell proliferation in Min6 using 5-bromo-2-deoxyuridine (BrdU)

BrdU is a proliferation assay that can be applied to evaluate whether the cells are actively dividing cells or not via the use of a specific labeling reagent. The BrdU labeling reagent (Life Technology, Paisley, UK) is a thymidine base analogue. The principle behind this technique can be summarized as follows.

As the cells undergo cell division, they require nitrogen bases during DNA synthesis. Because the BrdU labeling reagent is a thymidine analogue, proliferating cells

incorporate it into the genetic material. This incorporation of the thymidine analogue can be detected using several detection methods such as immunofluorescence, flow cytometery and cytochemical techniques. However, the detection method used in this project was a fluorescently labeled antibody.

To set up the experiment, cells were trypsinized and counted as in Section 2.1.1 and 2.1.3 to be plated as 50,000 cells/well in 1 ml of medium were allowed to adhere and grow on sterile glass coverslips placed in the bottom of a flat-bottom 24-well plate for overnight. The next day, cells were treated with rapamycin 300 nM, 200 nM, 100 nM, 10 nM and DMSO control for 24 hours. Each condition was set in triplicates. Following treatment, cells were washed with pre-warmed PBS and then incubated with BrdU in culture medium for 2 hours according to manufacturer's instructions. The BrdU was replaced with fresh culture media and cells were allowed to grow overnight. Cells were washed twice with PBS prior to fixing with 4% formalin (Sigma, St. Louis, MO, USA) in PBS for 20-30 minutes. After washing the cells with PBS, antigen retrieval was done by immersing the coverslips in citrate buffer (Sigma, Dorset, UK). Then, the buffer was heated using a microwave for 2 minutes on medium power. Coverslips were carefully picked up and transferred back to the 24-well plate that contained fresh PBS to cool down the coverslips.

Cells were permeabilized using 0.1% Triton X-100 (Sigma, Dorset, UK) in PBS for 20-30 minutes. Then, the coverslips were covered with 10% normal goat serum (NGS) (Sigma, Dorset, UK) for 1 hour followed by applying Anti-BrdU antibody (Bio-Rad, UK), (1:200 in PBS containing 3% NGS) and incubated overnight. The following day, coverslips were washed with PBS and incubated with the secondary fluorescently labeled antibody (Abcam, Cambridge, UK) (same condition as the primary antibody) for 1 hour.

Finally, coverslips were washed three times with 0.1% Tween-20 (Sigma, Dorset, UK) in PBS and mounted with ProLong DAPI (Life Technology, Paisley, UK) onto a frosted end microscopic slide. DAPI was used as both mounting media and nuclear stain. Slides were viewed at the Imaging Core Facility (University of Manchester, Faculty of Life Sciences) using Olympus BX51 upright fluorescent microscope connected to a CoolSnap camera (Photometrics, UK). Images were captured using

MetaVue Software (Molecular Devices, Berkshire, UK). Following image capture, images were viewed using ImageJ software.

2.4 Effect of rapamycin on apoptosis

Cells were checked for apoptotic events by assessing caspase 3/7 activity in cells incubated with 200 nM of rapamycin using Caspase-Glo 3/7 assay (Promega).

To set up the experiment, cells were trypsinized and counted as in Section 2.1.1 and 2.1.3 to be plated as 5000 cells/well in 100 µl of medium in a white-walled, clear bottom 96-well plate. Cells were allowed to grow overnight at 37^0C in a humidified incubator supplemented with 5% CO_2. The conditions used in this assay were untreated *vs.* DMSO control *vs.* 200 nM rapamycin *vs.* 5 µM cisplatin (positive control).

The Caspase-Glo 3/7 assay (Promega, UK) measured the luminescence of the caspase 3/7 activity in cells. The assay was performed in a one-step fashion. The Caspase-Glo 3/7 reagent in the kit consisted of a proluminescent substrate in a lysing solution containing luciferase. The reagent was added directly to wells in a 1:1 ratio to lyse the cells. Activated caspases in the lysed cells cleaved the substrate in the solution generating a luminescent signal. The luminescence signal was recorded using a Synergy HT plate reader and its Gen5 software (BioTek, Vermont, USA). The plate reader was set to luminescent mode and luminescence reading was measured without filtering the signal according manufacturer instructions.

2.5 Effects of rapamycin treatment on changes in ATP level

Intracellular ATP concentration was assessed using CellTiter-Glo assay from Promega. To set up the experiment, cells were trypsinized and counted as in Section 2.1.1 and 2.1.3 to be plated as 50,000 cells/well in 100 µl of medium in white-walled, flat, clear bottom 96-well plate. Cells were allowed to grow overnight at 37^0C in a humidified incubator supplemented with 5% CO_2. In this assay cells were treated with rapamycin for 1 or 2 hours to assess changes in ATP concentration. Following treatment with rapamycin CellTiter-Glo reagent was added directly to cells in a 1:1 ratio according to manufacturer's instructions. The reagent containing luciferase lysed the cells and ATP was released from the cell into the lysate. Luminescent signal was generated and signal was proportional to the amount of ATP in presence. A standard

curve was generated using ascending concentrations of ATP (0-10 μM). The luminescence signal was recorded using a Synergy HT plate reader and its Gen5 software (BioTek, Vermont, USA). The plate reader was set to luminescent mode and luminescence reading was measured without filtering the signal according manufacturer instructions.

2.6 RNA extraction and reverse transcription

RNA was extracted and purified from Min6 cells once they reached 50-60% confluence on T25 flasks (passages 19 and 22) using Qiagen RNeasy Mini Kit and RNase-Free DNase set following the manufacturer's instruction. According to the manufacturer's data, the RNA was released from the RNeasy membrane using RNase-free water. The extracted RNA was quantified NanoDrop 2000 Spectrophotometer (Thermo Scientific, UK).

Next, the extracted RNA was then reverse transcribed (RT) into complementary DNA (cDNA) using nanoScript and nanoScript 2 Reverse Transcription kit by Primerdesign (Southampton, UK) following manufacturer's instructions. A negative control sample was prepared using RNA with no NanoScript/NanoScript 2 enzyme added (RT negative control, -RT). The cDNA produced by RT was stored at -20°C prior to usage.

2.6.1 Primer design

All the cDNA sequences for the genes in this project were obtain from the National Centre for Biotechnology Information (NCBI) website (http://ncbi.nlm.nih.gov/gene). The primers in this project were selected using "pick primers" function on the mentioned website when gene of interest was selected. Primer specificity was checked using the Primer-BLAST function on NCBI website (https://www.ncbi.nlm.nih.gov/tools/primer-blast). PCR primers for mouse cDNA sequences were ordered from Eurofins Genomics (Derby, UK). Primer sequences, annealing temperatures and expected product sizes used in this project are listed in Table 1. The annealing (melting) temperature for both primers were calculated using the formula:

$T_m = 4(G + C) + 2(A + T)$ °C.

2.6.2 Polymerase Chain Reaction and gel electrophoresis

After acquiring the cDNA, two sets of samples were prepared, in addition to the mouse genetic DNA (gDNA) control: one set contained the cDNA samples, while the other set contained no polymerase (RT negative control). Each reaction contained a total volume of 25 µl as follow: 2.5 µl of 10x PCR buffer, 0.75 µl of $MgCl_2$, 0.5 µl of dNTPs, 0.625 µl of forward primer and 0.625 µl of reverse primer, 0.2 µl *Taq* DNA polymerase, 2 µl of template and 17.8 µl of autoclave distilled water. Final concentrations of reagents were therefore: 1.5 mM $MgCl_2$, 0.5mM forward primer, 0.5 mM reverse primer and 0.2 mM dNTPs.

The PCR conditions were as follows: 25-35 cycles of denaturation at 94°C for 45 seconds, annealing for 30 seconds according to Table 1 and elongation at 72°C for 90 seconds. An extra 10 minutes were added for extended elongation and finally termination at 4°C.

Lastly, the amplicon was applied to 2% agarose gel by BioLine (Taunton, MA, USA) by adding 2 g of agarose powder to 100 ml of Tris acetate Ethylene Diamine Triacetic Acid (TAE) buffer. The content was mixed and heated for 5 minutes using a microwave oven. For visualization of PCR product, 12 µl of GelRed™ (Biotium, Hayward, CA, USA) was added to the gel before adding the gel into the gel tray. After the gel solidified, it was transferred to electrophoresis chamber and submerged with TAE buffer.

A mixture of 5 µl of the amplified PCR product and 2 µl of loading dye were applied in each well, and run for 60-80 minutes at 110 V. The ladders used were 50 bp ladder (Invitrogen, UK) (for *insulin* and *Pdx1*) and Fast DNA ladder (New England Biolabs, Hertfordshire, UK) (for the *mTOR* components).

Images were then visualized and captured via a camera in a Bio-Rad ChemiDoc MP System (Hertfordshire, UK). Captured images were exported using Image Lab Software (Hertfordshire, UK). Captured images showed the amplified PCR products as white bands on a black background. The band sizes were measured by comparing to the bands of the amplified PCR products to the bands of the ladder used.

Primer name	Sequence (`5-3`)	T_m	Product size
Ms Insulin F	TCAAGCAGCACCTTTGTGGT	59^0C	127bp
Ms Insulin R	AGCTCCAGTTGTGCCACTTGT		
Ms PDX1 F	CAGTGGGCAGGAGGTGCTTA	62^0C	157bp
Ms PDX1 R	AGTTCAACATCACTGCCAGCTC		
Ms mTOR F	TGGGCCAACATGGCTAAGAG	62^0C	177 bp
Ms mTOR R	TCCCTCCCTCACTGAACACA		
Ms Deptor F	GCACATTGATCCAAACGCCA	61^0C	162 bp
Ms Deptor R	CATGCGTTCCAGCTCTCTCT		
Ms Raptor F	ACCATCCACTTGCCCAGATG	62^0C	350 bp
Ms Raptor R	GAGCAGGTCCTGTCGGAAAA		
Ms Rictor F	CTCAGCAAGCTCCCACATCA	63^0C	288 bp
Ms Rictor R	AGGGACTGGGCTCTTCTAGG		
Ms mLST8 F	GATTCCACGCTTCTTGCCAC	62^0C	410 bp
Ms mLST8 R	ACTGGCCTGACATGCTAACC		
Ms PRAS40 F	GCGGGCAATTCGAAACAGTA	63^0C	357 bp
Ms PRAS40 R	GCGCTGCAGTCAGTAATACC		
Ms Protor F	GCGAGCCATGGTTCACAGG	63^0C	352 bp
Ms Protor R	GATGAAGAGCTCCTGGTCGG		
Ms mSin1 F	CGTCTTGCAGATCGGGGACT	63^0C	288 bp
Ms mSin1 R	TATGTAGCCCTGCGTCTCAC		

Table 2.1: Primers sequences, calculated T_m and expected product size.

2.7 Immunofluorescence labelling of Min6 cells

In addition to the PCR, immunofluorescence was performed to confirm that the Min6 cell line had insulin protein expression. Cells were trypsinized and counted as in Section 2.1.1 and 2.1.3. A total of 50,000 cells/well in 1 ml of medium were allowed to adhere and grow on sterile glass coverslips placed in the bottom of a flat-bottom 24-well plate. Cells were fixed, permeabilized, stained, coverslipped as in Section 2.3. The primary antibody (Life Technology, Paisley, UK) and secondary fluorescently labelled antibody (Life Technology, Paisley, UK) were applied as in Section 2.3. Negative control was included by adding the secondary antibody, but not the primary antibody.

Slides were viewed and images were taken at the Bioimaging Core Facility (University of Manchester, Faculty of Life Sciences) using a microscope attached to CoolSnap camera and MetaVue software for imaging. Finally, the images were examined using ImageJ software.

2.8 Measurement of insulin secretion from Min6 cells

To set up the experiment, a 50-60% confluent T25 flask of Min6 cell (passage 19-32) was trypsinized and counted as in Section 2.1.1 and 2.1.3 to seed 20,000 cells/well in 1 ml of medium in a 24-well plate (each treatment was done in triplicate, with an additional three wells used for cell count to confirm the number of cells/well). The cells were incubated overnight to permit attachment to the wells. The following day, cell culture medium was removed and replaced with 1 ml Krebs Ringer Phosphate HEPES Buffer (KRH) containing 2 mM glucose (the final concentrations of KRH buffer components were: 129 mM NaCl, 4.8 mM KCl, 1.2 mM $MgSO_4.7H_2O$, 1.3 mM $Na_2HPO_4.2H_2O$, 1.2 mM KH_2PO_4, 2.5 mM $CaCl_2.2H_2O$, 4.17 mM $NaHCO_3$, 10 mM HEPES and 0.1% bovine serum albumin (BSA), pH 7.5) for 1 hour.

After the cells were incubated in KRH buffer containing the 2 mM glucose for 1 hour at 37^oC in a humidified 5% CO_2 in air incubator, to allow basal levels of insulin secretion to be established, the buffer was removed and discarded. Then, the required condition was added to each well and incubated for 30 minutes containing either 2 mM glucose or 20 mM glucose. After 30 minutes supernatants were collected, centrifuged at 1700 g for 5 minutes using a benchtop Minispin Plus microcentrifuge (Eppendorf, Histon, UK), aliquoted and frozen at -20^0C until analysis.

Insulin concentration was measured using ALPCO Mouse Insulin ELISA (ALPCO Diagnostics, Salem, NH, USA). Each set of experiment was repeated 3-4 times using different passage number with 3-4 biological replicates for each treatment. ELISA was carried out for each well in triplicates and average was taken for those technical replicates to represent one well.

The conditions used in this project were designed to evaluate insulin secretion in response to glucose (Glucose-Stimulated Insulin Secretion (GSIS) mechanism), or alternative receptor-based initiation of insulin secretion, in the absence and presence of rapamycin (200 nM; Stratech Scientific Limited, Suffolk, UK).

Insulin secretion stimulators used were 100 µM each of adenosine triphosphate (ATP), uridine triphosphate (UTP) and Acetylcholine (ACh) all from (Sigma, Dorset, UK), in buffer containing 2 mM glucose.

2.9 Measuring changes in $[Ca^{2+}]_i$ in Min6 cell channels using FlexStation 3

FlexStation 3 (Molecular Devices, Berkshire) was used to detect $[Ca^{2+}]_i$ changes in Min6 cells when stimulated with different conditions. To set up the assay, 60-70% confluent T25 flask of Min6 cell line (passage 20, 25, 32) was trypsinized and plated into a 96-well black-wall, clear- bottom plate as in Sections 2.1.1 and 2.1.3 to plate 50,000 cells/100µl/well.

Cells were allow to grow overnight and the compound plate containing the required treatment conditions was prepared fresh on the day of the assay and pipetted into a v-bottom 96-well plate. All the tested conditions were prepared 3 times (3x) the required concentration due to the difference in transferred volume by the machine used. For example, 40 mM KCl, used in high KCl condition, was prepared as 120 mM, because the machine transferred 50 µl of 120 mM KCl to 100 µl loaded cells. The composition of the KRH used was similar to the one used in Section 2.7.

Next, a fresh aliquot of Calcium 6 or Calcium 6-QF loading dye (Molecular Devices, Berkshire) was prepared according to manufacturer's instructions. Then, 100 µl of loading dye was added to all the wells and incubated for 2 hours at 37^0C incubator. Finally, the compound and loaded cells were inserted into the FlexStation 3 machine (Molecular Devices, Berkshire) for assay using manufacturer's Calcium 6 or Calcium 6-QF protocol. Data were analyzed and exported using version 5.6 of Softmax Pro software (Molecular Devices, Berkshire, UK). The settings used in this experiments were according to manufacturer instructions.
The peak values analysis of the data were produced by Softmax Pro software.

2.10 Statistical analysis

Data obtained were presented as mean ± standard error of the mean (SEM). Data were statistically analyzed using a free version of GraphPad Prism 6 software (California, USA). D'Agostino-Pearson normality test was applied to check if the data obtained were normally distributed. Comparisons were made using Two-way analysis of

Variance (ANOVA) followed by Dunnett's post-hoc test for Section 2.2, Student's t-test for Section 2.4, one-way ANOVA followed by Tukey's post-hoc test for Section 2.7 and 2.8 and one-way ANOVA followed by Dunnett's post-hoc test for Section 2.3. P value of less than 0.05 was considered as significant.

Chapter 3:

Results

3.1 Expression of *PDX1* and *INS* genes in Min6 cells

Min6 cell lines secrete insulin in a glucose-dependent manner, and PDX1 is a key transcription factor involved in the glucose-dependent activation of the insulin promoter (Miyazaki et al, 1990; Macfarlane et al, 1999). Therefore, RT-PCR was performed to confirm the expression of *INS* and *PDX1* genes (Fig 3.1). The products of both RT-PCRs were run on a 2% agarose gel with a 50 base pair (bp) ladder to examine the product size. The gel showed clear bands for *PDX1* and *INS* measured as 157 bp and 127 bp for *PDX1* and *INS* respectively.

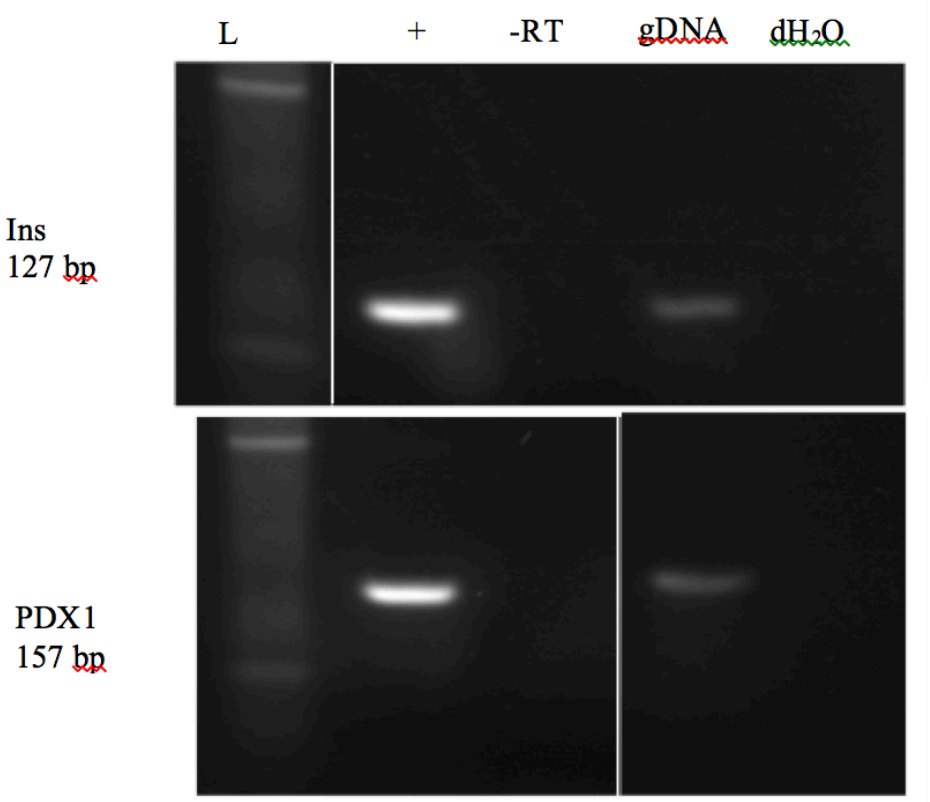

Figure 3.1: *INS* and *PDX1* gene expression in Min6 cells via RT-PCR and visualised in 2% agarose gel. The RT-PCR was done on Min6 p18 with a total n=3. GelRed was used for visualization. Insulin size was 127 bp while Pdx1 was 157 bp; L = ladder, Ins = Insulin, + = Min6 p18, -RT = Reverse transcriptase negative control; gDNA = mouse Insulin genomic DNA

3.2 Min6 express genes encoding all mTOR components

Before studying the physiological effects of rapamycin, cells were assessed for the gene expression of mTORC1 (mTOR, RAPTOR, DEPTOR, mLST8 and PRAS40 subunits) and mTORC2 (mTOR, RICTOR, DEPTOR, mSIN1, Protor and mLST8 subunits) components by standard RT-PCR (Fig. 3.2).

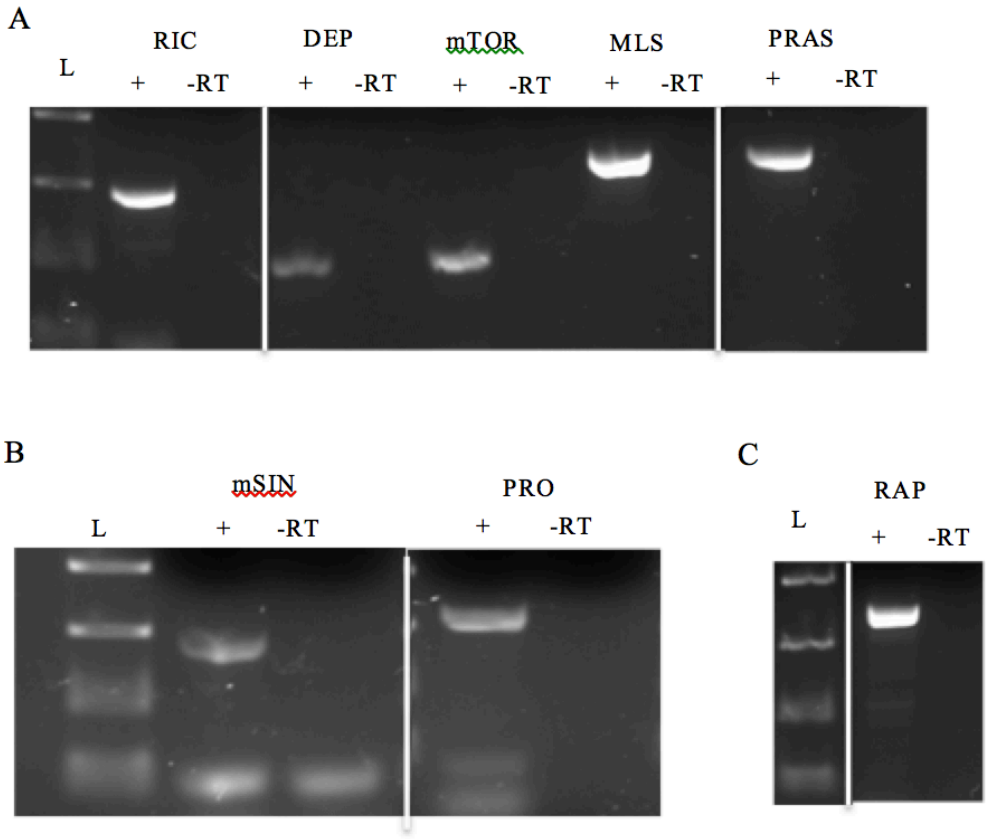

Figure 3.2: Min6 express all the components of mTORC1 and mTORC2 required for the action of rapamycin in 2% agarose gel. Panel A: correct band sizes were observed for RICTOR 288 bp, DEPTOR 162 bp, mTOR 177 bp, MLST8 410 bp and PRAS40 357 bp. Panel B: showed mSIN1 288 bp and Protor 352 bp. Panel C: showed RAPTOR 350 bp. (n=3); (RIC = RICTOR; DEP = DEPTOR; mT = mTOR; MLS = MLST8; PRAS = PRAS40; mSIN = mSIN1; PRO = PROTOR; RAP = RAPTOR; -RT = Reverse transcriptase negative control).

3.3 Expression of insulin protein in Min6 cells

Following confirmation of gene expression of *INS*, qualitative immunofluorescence of insulin was carried out on Min6 (passages 14, 17, 19 and 20) (Fig. 3.3). The cells showed positive cytoplasmic staining of insulin.

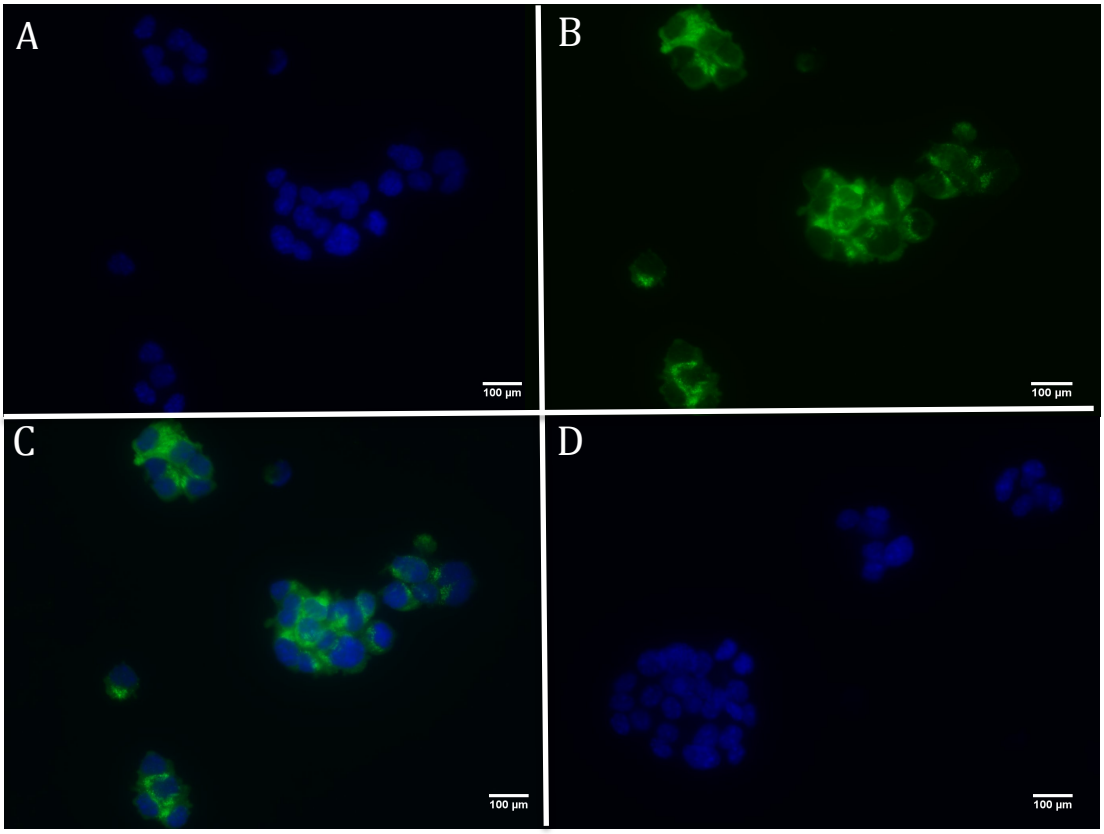

Figure 3.3: Expression of insulin protein in Min6 cells p17. Panel A shows nuclear staining of DAPI, while B displays staining of insulin. The digitally combined image of A and B can be seen in C. Panel D shows a combined DAPI/secondary antibody control with no primary antibody. (n=4); Scale bar 100 µm.

3.4 Rapamycin reduced cell proliferation rate

Fig.3.4 shows the effect of different concentrations of rapamycin (0-300 nM) on the proliferation rate of Min6 cells over 4-days. Cells were seeded at 50,000 cells/well/ml on day 0 in 24-well plates.

No significant difference in cell proliferation was observed for days 1 or 2 when comparing the control with rapamycin containing wells. On day 3, the control cell proliferation was almost doubled when compared to 300 nM rapamycin containing wells ($p \leq 0.05$). Statistical significance was observed on day 4 when comparing the control to all of the rapamycin containing wells ($p \leq 0.01$ when comparing the control to 300 nM, $p \leq 0.05$ when comparing the control to the rest of the concentrations used, i.e. 200 nM, 100 nM and 10 nM rapamycin containing wells).

The experiment was repeated four times, with triplicate wells in each experiment (n=4). Viability of cells was not clearly affected when cell count was performed using

trypan blue although there were problems with this method of detecting cell death, since dead cells may have been washed away during the protocol.

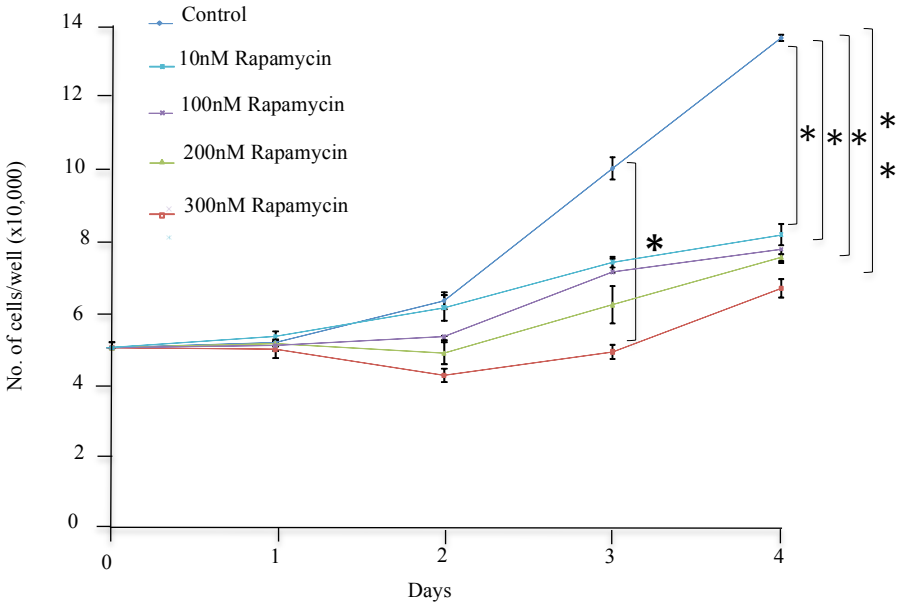

Figure 3.4: Rapamycin reduces cell proliferation over 4-days. Significant reduction in cell proliferation was apparent from day 3 relative to no treatment control ($p \leq 0.05$). On day 4 of the treatment, notable reduction in cell proliferation was observed ($p \leq 0.01$ when comparing the control to 300 nM, $p \leq 0.05$ when comparing the control to the rest). (* $p \leq 0.05$; ** $p \leq 0.01$ compared to untreated control cells; two-way ANOVA followed by Dunnett's post-hoc test; n=4 independent experiments).

Based on preliminary data, 200 nM rapamycin showed reduced cell proliferation in Min6 cells, by BrdU incorporation assay. However, this experiment was only completed once. Further experiments need to be done to draw any conclusions.

The next question was whether rapamycin induced apoptosis, since cell count was reduced, but cell death could not be detected by trypan blue exclusion.

3.5 Rapamycin did not have a detectable apoptotic effect on Min6 cells

Min6 cells were treated with 200 nM rapamycin for 3 days. Then the Caspase-Glo reagent was added and luminescence was read according to manufacturer's instructions. A positive control (5 μM cisplatin) was added to ensure that caspase cascade activation could be detected by the assay. Comparisons were made using One-way ANOVA followed by Dunnett's post-hoc test. P values of less than 0.05

were considered as significant. Although the positive control showed caspase activity, no statistical significant differences were found when comparing rapamycin treated cells with DMSO control or untreated cells.

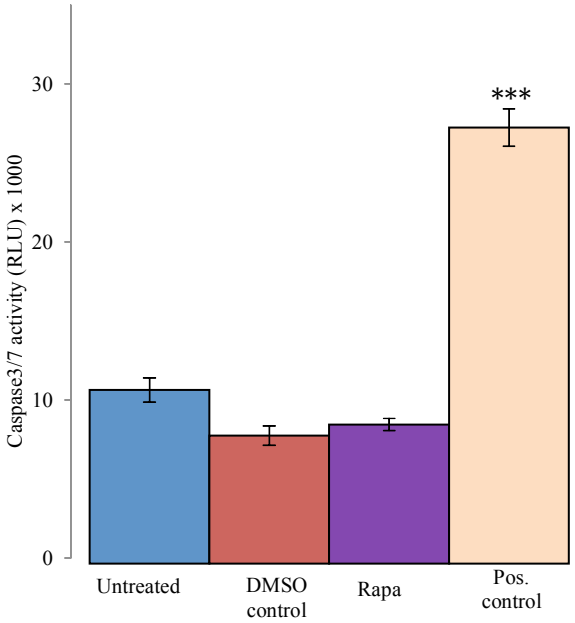

Figure 3.5: Rapamycin treatment (3 day) is not associated with apoptosis involving caspase-3 or -7. Caspase-3 and -7 activity was not increased by 3-day treatment with Rapa (rapamycin (200 nM), or DMSO vehicle control, suggesting that treatment does not induce apoptosis. (*** $p \leq 0.001$ compared to DMSO control cells; one-way ANOVA followed by Dunnett's post-hoc test; n=4 independent experiments); Pos. control=5 µM cisplatin.

3.6 Rapamycin (200 nM) reduced insulin secretion under stimulated conditions

In Fig.3.6, cells were stimulated to secrete insulin secretion by 2 methods: I. by triggering K_{ATP} channel dependent signaling (using glucose), which involves Ca^{2+} entry via Voltage dependent Calcium channel and II. by stimulating purinergic and muscarinic receptors on β-cell membrane to invoke Ca^{2+} release from intracellular stores.

Significant insulin secretion was observed when comparing 2 mM glucose (control) to 20 mM glucose ($p \leq 0.05$). Also enhanced insulin secretion was observed when ATP, UTP and ACh (100 µM each) were compared to 2 mM glucose ($p \leq 0.001$, $p \leq 0.01$, $p \leq 0.001$, respectively) (n=3). However the enhanced insulin secretion was reduced when rapamycin (200 nM) was added to 20 mM glucose in (Fig. 3.7). The stimulator mix of ATP, UTP and ACh (100 µM of each; Fig.3.8) was added to get a robust insulin secretion from Min6 by stimulating both purinergic and muscarinic receptors, and to check if rapamycin was capable of reducing the receptor stimulated insulin

secretion. However, it was not determined in this experiment if rapamycin inhibits both receptors, as Fig. 3.8 showed that the effect could be exerted on either one. Individual components should be assessed to draw final conclusion. Rapamycin did not reduce basal insulin secretion, and did not reduce stimulated secretion below basal insulin secretion levels (Figs. 3.7 and 3.8).

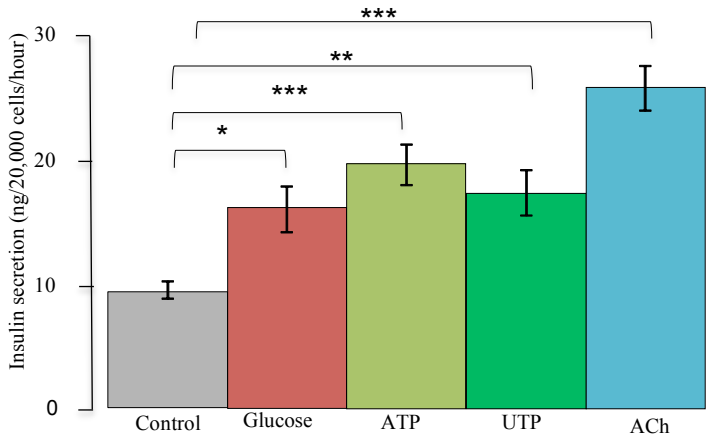

Figure 3.6: Insulin secretion in Min6 cells. Insulin secretion was increased when stimulated with 20 mM glucose, ATP, UTP and ACh (100 µM each). Statistical significant was found when comparing the control with glucose ($p \leq 0.05$), ATP ($p \leq 0.001$), UTP ($p \leq 0.01$) and ACh ($p \leq 0.001$). (* $p \leq 0.05$; ** $p \leq 0.01$; *** $p \leq 0.001$ compared to control cells; one-way ANOVA followed by Tukey's post-hoc test; n=9 independent experiments).

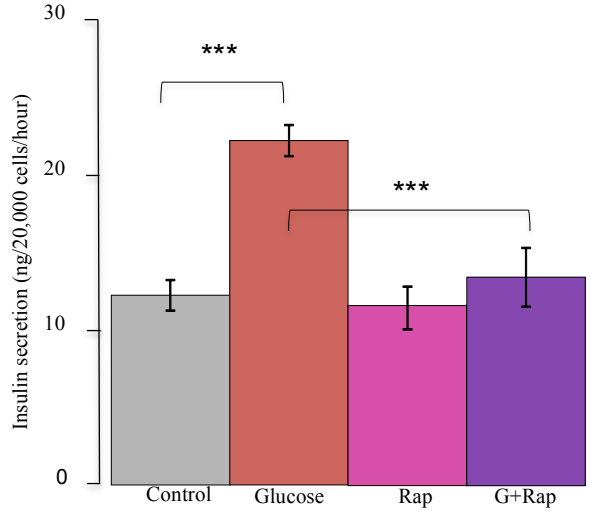

Figure 3.7: Rapamycin inhibits glucose stimulated insulin secretion. Although rapamycin reduced glucose-stimulated insulin secretion, there were no effects on basal, unstimulated secretion. Significant differences were found when comparing the control with glucose (***$p<0.001$) and when comparing the glucose with glucose + rapamycin (***$p<0.001$). (***$p<0.001$ compared to control cells; one-way ANOVA followed by Tukey's post-hoc test; n=24 independent experiments). Rap, rapamycin (200 nM); G+Rap, glucose (20 mM) + rapamycin (200 nM).

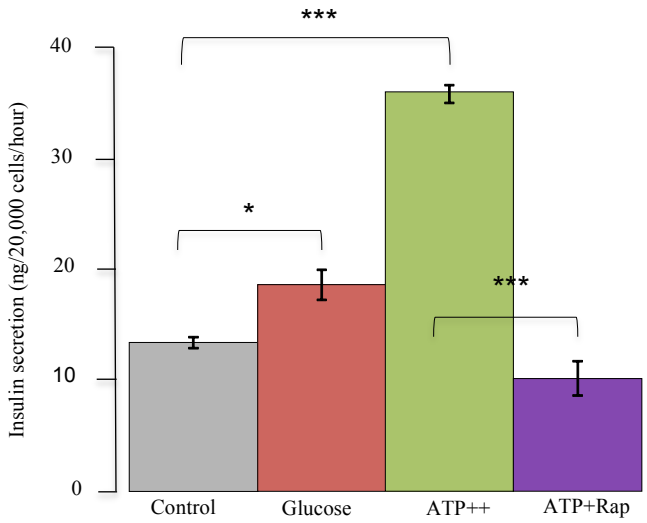

Figure 3.8: Rapamycin inhibits receptor stimulated insulin secretion from Min6. Stimulation of insulin secretion by a mixture of ATP, UTP and ACh (100 µM each, ATP++) was inhibited by rapamycin (200 nM). Significant differences were found when comparing the control with glucose ($p \leq 0.05$), the control with ATP++ ($p \leq 0.001$) and ATP++ with ATP + rapamycin. (*$p \leq 0.05$, *** $p \leq 0.001$ compared to control cells; one-way ANOVA followed by Tukey's post-hoc test; n=9 independent experiments).

Fig. 3.9 shows the effect of the K_{ATP} channel activator diazoxide (200 µM), which is the standard drug used for CHI therapy. Diazoxide treatment reduced GSIS ($p \leq 0.001$). Diazoxide reduced glucose-induced insulin secretion back to basal levels. The experiment was repeated 5 times (n=20).

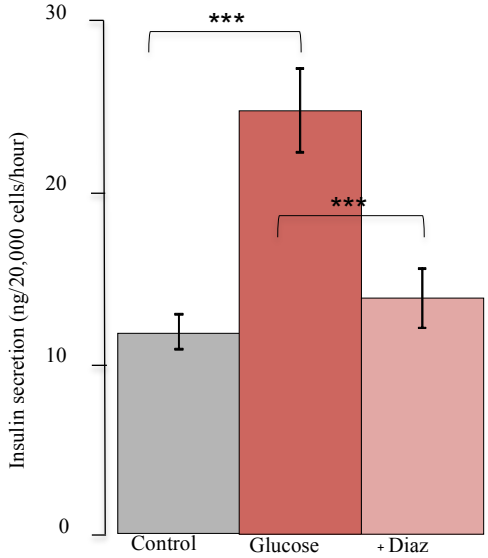

Figure 3.9: Diazoxide (200 µM) inhibits 20 mM glucose-stimulated insulin secretion in Min6 cells. Statistical significance were found when comparing the control with glucose ($p \leq 0.001$) and glucose with + diazoxide ($p \leq 0.001$). (*** $p \leq 0.001$ compared to glucose-treated cells; one-way ANOVA followed by Dunnett's post-hoc test; n=20 independent experiments); + Diaz, 20 mM glucose + 200 µM diazoxide

In order to determine how readily reversible the actions of rapamycin were, cells were pre-incubated with rapamycin for one hour, followed by variable recovery times prior to assessing GSIS. Fig. 3.10 shows that the preincubation of Min6 cells with rapamycin (200 nM) for 1 hour was enough to prevent insulin secretion in wells containing 20 mM glucose ($p \leq 0.001$). Although the cells were allowed to recover for 1 hour in fresh culture media, this did not ameliorate the inhibitory effect of rapamycin. The experiment was repeated 3 times ($n=12$).

Next, Min6 cells were preincubated with rapamycin (200 nM) for 1 hour, but were allowed to recover in fresh culture media for 6 hours instead of 1 hour (Fig. 3.11). However, the effect of rapamycin was not reversible.

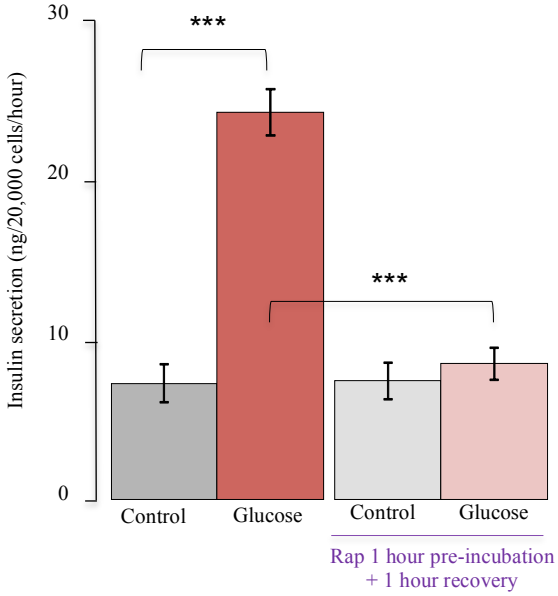

Figure 3.10: Effects of short pre-incubation with rapamycin are not reversed in 1 hour. Following 1 hour pre-incubation of cells with rapamycin (200 nM) and 1 hour recovery, inhibition of 20 mM glucose-induced insulin secretion was maintained. Significant changes were found when comparing the control to glucose ($p<0.001$) and glucose to the pre-incubated glucose ($p<0.001$). (***$p<0.001$ compared to control cells; one-way ANOVA followed by Tukey's post-hoc test; n=12 independent experiments).

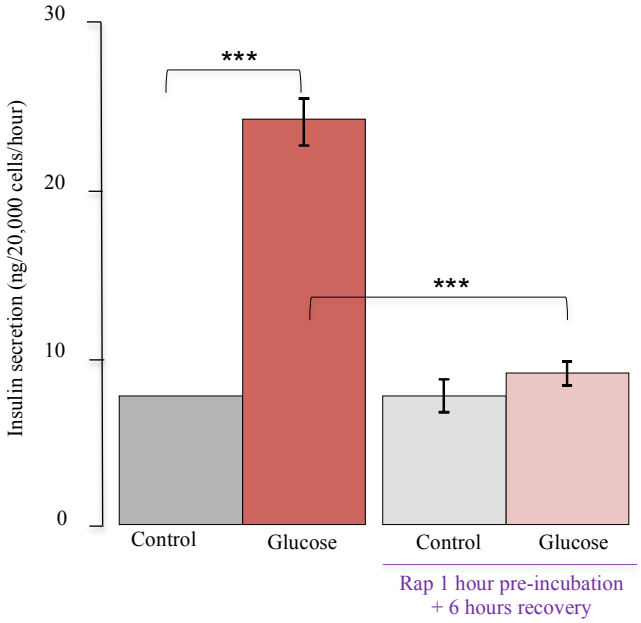

Figure 3.11: Effects of short pre-incubation with rapamycin are not reversed in 6 hours. Following 1hr. pre-incubation of cells with rapamycin (200 nM) and 6 hour recovery, inhibition of 20 mM glucose-induced insulin secretion was maintained. Significant changes were found when comparing the control to glucose ($p<0.001$) and glucose to the pre-incubated glucose ($p<0.001$). (***$p<0.001$ compared to control cells; one-way ANOVA followed by Tukey's post-hoc test; n=12 independent experiments).

Lastly, Min6 cells were preincubated with rapamycin (200 nM) for 3 days, and allowed to recover in fresh culture medium for 6 hours instead of 1hour (Fig. 3.12). This experiment showed similar results to the previous preincubation experiments (Figs. 3.10 and 3.11), in that the effect of rapamycin was not reversible.

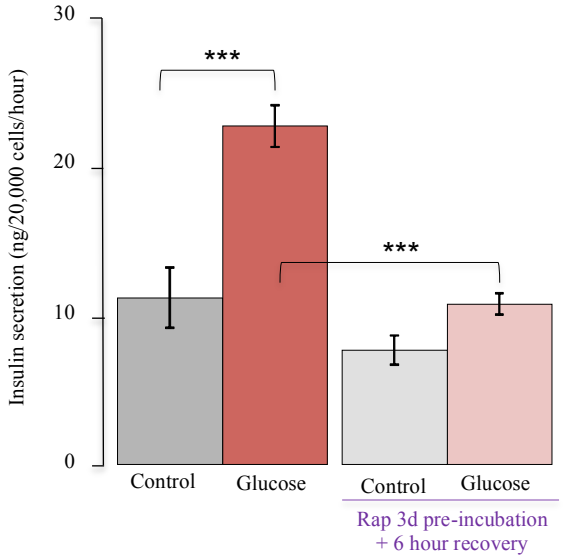

Figure 3.12: Effects of long pre-incubation with rapamycin are not reversed in 6 hours. Following 3 day pre-incubation of cells with rapamycin (200 nM) and 6 hour recovery, inhibition of 20 mM glucose-induced insulin secretion was maintained. Significant changes were found when comparing the control to glucose ($p<0.001$) and glucose to the pre-incubated glucose ($p<0.001$). (***$p<0.001$ compared to control cells; one-way ANOVA followed by Tukey's post-hoc test; n=6 independent experiments).

3.7 CellTiter-Glo assay failed to detect changes in ATP level

As mentioned earlier in Section 1.3, the increase in intracellular ATP/ADP ratio leads to the closure of K_{ATP} channels, which starts the pathway that eventually causes insulin exocytosis. As rapamycin affects ATP production (Barlow et al., 2013; Morita et al., 2013), we wanted to test if rapamycin (200 nM) treatment would change the level of ATP production in Min6 cells using CellTiter-Glo assay by Promega. The reagent was added directly to the cells according to manufacturer's instructions and readings were taken after 1 hour and 2 hours of treatment with rapamycin.

Following the first hour of treatment with rapamycin, no significant changes were observed when comparing the control with rapamycin (Fig. 3.13). Also no significant changes were found when comparing control, with rapamycin treated cells after 2 hours. However, this experiment was attempted only once (n=1) and did not include a positive control for the assay. Therefore, further investigation is required to evaluate the effect of rapamycin on ATP production.

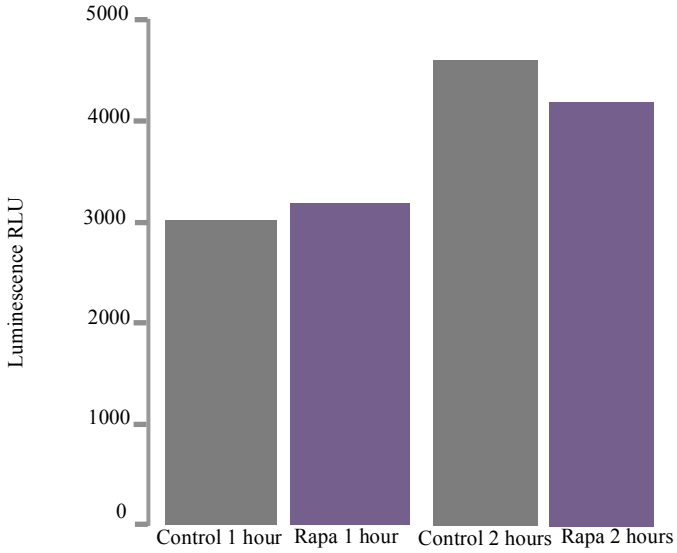

Figure 3.13: No changes in ATP level was observed with rapamycin treatment. CellTiter-Glo assay failed to detect any changes between the control or rapamycin treatment. Comparisons were made using Student's t-test; (n=1); Rap, 200 nM rapamycin.

3.8 Rapamycin does not prevent increases in intracellular Ca^{2+} levels following stimulation of purinergic and muscarinic receptors

Since preliminary experiments indicated that rapamycin did not significantly affect ATP levels, we wanted to test if rapamycin had an effect on $[Ca^{2+}]_i$, because changes in $[Ca^{2+}]_i$ are initiated following ATP generation (which closes K_{ATP} channels, causing membrane depolarization and activation of voltage-dependent Ca^{2+} channels) as mention earlier in Section 1.3. Cells were stimulated with 20 mM glucose, ATP + UTP (100 μM each), ACh (100 μM) and KCl (40 mM) vs. the same conditions containing 200 nM rapamycin, and changes in $[Ca^{2+}]_i$ monitored using a fluorescent plate reader (FlexStation3; Fig. 3.14). Although, the cells did not show significant changes when stimulated with 20 mM glucose, notable changes in $[Ca^{2+}]_i$ peak fluorescence were observed when cells were stimulated with the other conditions (with and without rapamycin).

The purinergic receptor stimulators ATP and UTP, as well as KCl, showed significant changes ($p \leq 0.0001$) in peak florescence compared to the control. ACh, and ACh with rapamycin also showed significant changes ($p \leq 0.001$, $p \leq 0.01$) in $[Ca^{2+}]_i$ peak florescence when the muscarinic receptor was stimulated.

Interestingly, when rapamycin (200 nM) was added to receptor stimulators (ATP + UTP and ACh) and the depolarizing solution KCl (40 mM), no significant effect was observed on $[Ca^{2+}]_i$ level (Fig. 3.14 Panel B). These data suggest that rapamycin did not influence changes in intracellular $[Ca^{2+}]_i$ brought about by different stimulators of insulin release.

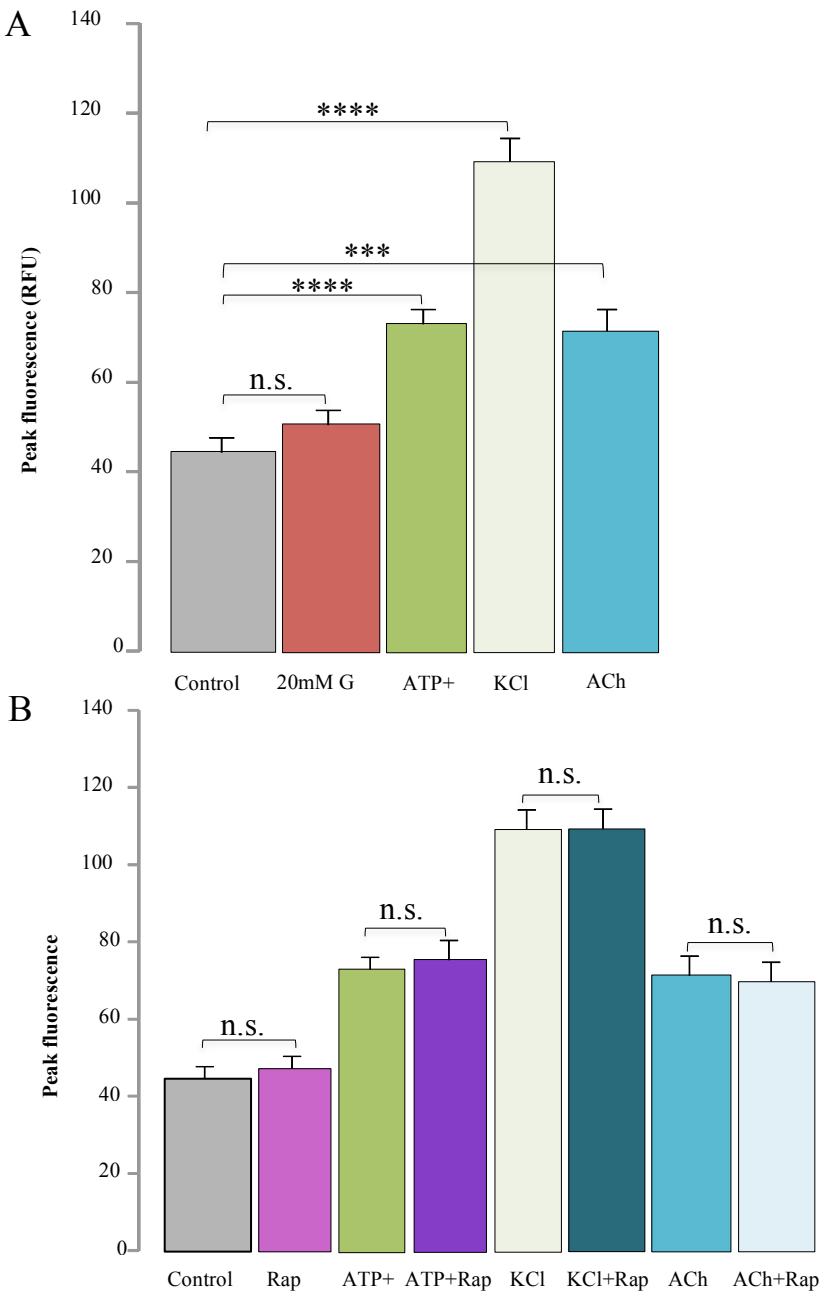

Figure 3.14: Rapamycin does not prevent changes in $[Ca^{2+}]_i$ level.

Panel A. Significant changes in Ca^{2+} level were noted when stimulated with ATP + UTP, KCl and ACh.

Panel B. Rapamycin did not prevent changes in $[Ca^{2+}]_i$ brought about by ATP + UTP, ACh and KCl. (**$p \leq 0.01$; ***$p \leq 0.001$; ****$p \leq 0.0001$ compared to control cells; one-way ANOVA followed by Tukey's post-hoc test; n=3 independent experiments). Rap, rapamycin (200 nM); ATP+, ATP + UTP (100 μM each); ATP+Rap, ATP + UTP (100 μM each) + rapamycin (200 nM); ACh, Acetylcholine (100 μM); ACh+Rap, Acetylcholine (100 μM) + rapamycin (200 nM); n.s., not significant.

Chapter 4:

Discussion

4.1 Min6 cells expressed *PDX1, insulin* and all the components of mTOR complexes

PDX1 expression in β-cells plays a role in maintaining cell mass, function and survival, as well as the expression of insulin (Szabat et al., 2012). The expression of *PDX1* occurs when cells become committed to a pancreatic lineage, and continues throughout the differentiation into β-cells (Szabat et al., 2012). Our data showed that *PDX1* and *insulin* gene expression in Min6 cell line was consistent at passage 18, 20 and 22 (Fig. 3.1); passages used extensively during this study. The importance of *PDX1* and *insulin* genes to β-cells identity and function has been reported previously (Szabat et al., 2010, Khoo, 2011, Gao et al., 2014). The deletion of *PDX1* alone was associated with reduced β-cell mass and increased cell death (Li et al., 2005; Szabat et al., 2012), suggesting that *PDX1* is not only pivotal for β-cell identity and function but also maintenance of the β-cell mass to cope with body demands. In the context of this study, expression of key murine genes involved in insulin secretion helped to confirm the identity of the cell line prior to further experimentation, in the absence of DNA fingerprinting techniques (Katsnelson, 2010).

The mTOR exists as two complexes: mTORC1 (mTOR, DEPTOR, RAPTOR, PRAS40 and mLST8) and mTORC2 (mTOR, DEPTOR, RICTOR, Protor, mSIN1 and mLST8) (Pópulo et al., 2012). Our PCR data confirmed the gene expression of all the components required for the action of rapamycin in Min6 cells, as reported previously (Pópulo et al., 2012). Despite this, it is well reported that protein expression does not always match mRNA expression due to variations in mRNA stability, mRNA translation efficiency and post-translational regulation (Kendrick, 2012).

The protein expression of components has not been fully investigated. Whilst, mTOR, RAPTOR and RICTOR are expressed at the protein level in Min6 (Barlow et al., 2012) other components have not been studied. Furthermore, the role of some components (e.g. Protor) is not clear (Laplante and Sabatini, 2009). Further investigation is required to elucidate the role of individual components in the responses to rapamycin treatment. Unfortunately, we were not able to study the protein expression due to lack of well-characterized antibodies and the time required for optimization.

4.2 Rapamycin reduced the cell count over 4 days with no increase in apoptosis

Rapamycin is an immunosuppressive drug that is used following transplant of organs and islets of Langerhans to treat type-1 diabetes (Bruni et al., 2014). The drug is also known to have an antiproliferative effect exerted on many cell types including β-cells (Zahr et al., 2008).

We expected to observe lower cell count numbers following treatment with rapamycin (Fig. 3.4). On days 3 and 4, Min6 cells growing in rapamycin containing media (10 nM - 300 nM) showed significantly lower cell number when compared control. A reduced cell count could be due to reduced cell proliferation, increased cell death, or a combination of both.

Manual cell count is an indirect method for assessing cell proliferation. The technique is also subjective due to technical errors such as mixing and pipetting errors, which influence the accuracy and precision of cell count. However, other techniques have been considered in the project to assess cell proliferation such as bromodeoxyuridine (BrdU) incorporation assay. The technique is considered a direct technique to assess cell proliferation as it is based on incorporating a synthetic deoxyuridine base into the DNA of actively dividing cells (Hall and Levison, 1990). After incorporation of BrdU reagent, specific antibodies can be used to quantify the number of replicating cells.

In my study, it was technically difficult to optimize BrdU incorporation as well as quantify the number of actively dividing cells. The technique was successful for one set of Min6 cell experiments during optimization (data not shown). In that particular experiment, it was shown that rapamycin reduced BrdU incorporation, suggesting that it inhibited proliferation, but with an n of 1, this was far from conclusive. Following attempts were not successful due to clumping of Min6 cells in tight cell clusters, which made interpretation of the data impossible. Although lower cell densities were also used (5000 cells/well/ml *vs.* 10,000 cells/well/ml), cell clusters were still present and the technique was not investigated further. Alternative techniques such as 5-ethynyl-2'-deoxyuridine (EdU) incorporation, and Ki-67 labelling would provide similar data to assess the effect of rapamycin on cell proliferation, but would also require prevention of cell clustering.

Our findings of reduced cell count after rapamycin treatment were similar to those reported previously in cells from different sources (human pancreatic ductal cells,

neonatal porcine islets, rat islets and porcine neonatal pancreas cell cluster) which all showed decreased proliferation rate, regardless of treatment duration (Bussiere et al., 2006; Sun et al., 2010; Niclauss et al., 2011; Barlow et al., 2013).

Proliferation is regulated by the mTOR pathway and its downstream proteins, which co-interact with a number of pathways such as PI3K and Akt pathway (see Fig 1.3). The overall result is an increase in production of nucleotides, proteins and lipids to aid cell growth (DeBerardinis et al., 2008; Ward and Thompson, 2012).

mTORC1 controls cell proliferation through phosphorylation and activation of its effector protein S6 Kinase 1 (S6K1) and phosphorylation and inactivation of eukaryotic initiation factor 4-binding protein (4E-BP1) (Hay and Sonenberg, 2004; Blandino-Rosano et al., 2012; Barlow et al., 2013; Schreiber et al., 2015). mTORC1 is negatively controlled by DEPTOR and PRAS40, as well as TSC1, TSC2, whereas RHEB (Ras homolog enriched in brain), a small G protein, positively regulates mTORC1 (Blandino-Rosano et al., 2012). There is general agreement that rapamycin treatment reduces or abolishes phosphorylation of Akt and S6K1 (Gleason et al., 2007; Ballou and Lin, 2008; Fraenkel et al., 2008), and this would likely contribute to the decreased proliferation observed in the Min6 cells.

Akt can also activate mTORC1 by two means: phosphorylating PRAS40 to remove its inhibitory action over mTORC1, and by phosphorylating TSC2 to prevent TSC1 and TSC2 complex formation (Blandino-Rosano et al., 2012). The prevention of TSC1 and TSC2 complex formation, activates Rheb that positively regulate mTORC1 (Blandino-Rosano et al., 2012; Pópulo et al., 2012).

Rapamycin, the mTOR inhibitor used in the present study, forms a complex with FKBP12 which then binds directly to mTORC1, but not to mTORC2 as reported in (Sarbassov et al., 2006; Shimobayashi and Hall, 2014). Beyond this interaction with FKBP12, the mechanism of action of rapamycin is less well known but could involve blocking of substrate recruitment via RAPTOR (Shimobayashi and Hall, 2014).
The role of mTORC2 in nucleotide, protein and lipid synthesis is less well understood, however it has been reported previously that rapamycin treatment for more than 24 hours leads to the dissociation of mTORC2 complex (Barlow et al., 2012; 2013). Therefore, although it was not assessed in the present study, it can be

expected that mTORC2 dissociation occurred in Min6 cells, which were treated with rapamycin for up to 4 days.

Additionally, mTOR controls control cell division and cell cycle progression (through mTORC1) from G_1 to S phase through 40S ribosomal protein S6K1 and 4E-BP1. Cyclin-dependent kinase is blocked by rapamycin and leads to more cyclin D1 turnover, and ultimately leads to deficiency of active cdk4/cyclin D1 complex (required for G_1 to S phase progression), which leads to cell cycle arrest (Hidalgo and Rowinsky, 2000).

4.3 Rapamycin did not cause detectable cell death

mTORC2 is responsible for cell survival by Akt through the PI3K pathway (Sarbassov et al., 2006). Continuous signaling by mTORC2 to Akt is pivotal for cell survival. However, treatment with rapamycin over 24 hours leads to dissociation of mTORC2 and decreased Akt phosphorylation (Sarbassov et al., 2006). Although cell viability was assessed throughout the experiment, trypan blue dye-exclusion failed to reveal the presence of cells undergoing cell death. However, this does not exclude the possibility of apoptosis because culture medium was changed on day 2 and it is possible that dying cells (which detach from the wells) would have been removed along with the old medium. As an alternative approach, we attempted to monitor apoptosis via caspase-3 and -7 activation using the Caspase-Glo 3/7 assay (Promega, UK).

There are two types of caspases: initiator, and effector caspases. Initiator caspases (such as caspase-8 and -9) activate effector caspases (caspases -3 and -7), which activate other caspases to dismantle dying cells (Cao et al., 2013). There are several pathways that could trigger caspase activation such as DNA damage, mitochondrial damage and membrane alteration (Elmore, 2007). In addition, some cells lack caspase-3 such as MCF-7 (Twiddy et al., 2006). These factors and more contribute to sensitivity of the assay.

Our data suggest that after treating the cells with rapamycin for 3 days, no significant changes in caspase-3 or -7 activity were observed when compared to the positive control (5 μM of cisplatin), and negative control (medium not supplemented with

rapamycin) (Fig. 3.5). This data implies that rapamycin, at the concentration used, over a period of 3 days did not cause apoptosis in Min6 cells. The outcomes of the assay were inconsistent with previous reports (Bell et al., 2003). Bell et al. (2003) exposed Min6 cells to rapamycin (10-100 nmol/L) for 19 hours and saw increased TUNEL-positive cells. Additionally, a recent study by Kloster-Jensen et al., (2016) showed that rapamycin treatment increased cell death when apoptosis was assessed using a different technique, the Cell Death Detection ELISA^{PLUS}.

Therefore, although our data implied that rapamycin did not cause cell death, further investigation is required due to conflicts with published literature. TUNEL assay is a direct and specific method to assess cell death via visualizing DNA breaks in cells undergoing DNA repair, using a fluorescent microscope. TUNEL would help to confirm whether or not rapamycin is toxic to β-cells as argued by some groups (Barlow et al., 2013).

Technical reasons that the Caspase-Glo assay may have not given accurate results in our hands include a lack of sufficient sensitivity of the assay (the positive control that was used causes high levels of cell death), or an effect due to different numbers of cells in each well tested. In future, manual cell counts could be performed to check for equal cell numbers in a parallel assay plate).

4.4 Rapamycin reduced insulin secretion from Min6 when added to 20 mM glucose and ATP/UTP/ACh

The Min6 cell line is known for sensing glucose, and secreting insulin accordingly in a glucose-dependent fashion and shares morphological features with normal β-cells (Miyazaki et al., 1990; Ishihara et al., 1993). Stimulating these cells with high glucose concentrations (20 mM), ATP, UTP and/or ACh (100 μM each), increases insulin secretion, via different mechanisms. However, at higher passages Min6 cells have been reported previously to lose their glucose responsiveness, whilst retaining responsiveness to other stimulators of insulin secretion (Miyazaki et al., 1990; Skelin et al., 2010; Cheng et al., 2012; Kobayashi et al., 2016). The loss of glucose-responsiveness has been explained by reduced gene expression of proteins involved in glucose metabolism (such as *Glut2*) (Minami et al., 2000), and those involved in insulin secretion, synthesis and possibly insulin transport (such as *Scgn, Gucy2c* and

Tmem59L) (Kobayashi et al., 2016).

All the insulin secretion experiments in this project were carried out in glucose responsive Min6 cells p23-p34. However, glucose responsiveness was lost later in the project, in Min6 cells used for investigation of changes in $[Ca^{2+}]_i$. Rapamycin reduced insulin secretion in Min6 to basal levels when it was added alongside high glucose (20 mM; Figs. 3.7, 3.10, 3.11 and 3.12). Similarly the Min6 cells had robust insulin secretion when stimulated with ATP, UTP or ACh ($p \leq 0.001$, $p \leq 0.01$, $p \leq 0.001$, respectively when compared with 2 mM glucose control) (Fig. 3.6); and the addition of 200 nM rapamycin to the mixture of ATP, UTP and ACh reduced insulin secretion back to basal levels ($p \leq 0.001$; Fig. 3.8). These data were consistent with experiments reported by (D'Amico et al., 2005; Barlow et al., 2012), in which rapamycin reduced GSIS in Min6 cells.

During our experiments, cells were exposed to rapamycin for 30 minutes; according to Barlow et al., 2012, this is most likely to lead to mTORC1 inhibition rather than mTORC2 inhibition which requires longer exposure times. There are a number of potential mechanisms behind the effects of mTORC1 inhibition on insulin secretion via crosstalk with other pathways, including PI3K-Akt signaling pathway (Barlow et al., 2013; Le Bacquer et al., 2013). Therefore, assessing intracellular Ca^{2+} levels, and assessing the activity of Glut-2 and key regulatory enzymes of glycolysis such as glucokinase, phosphofructokinase, and pyruvate kinase would help prove the involvement of theses processes of glucose metabolism.

Insulin secretion by ATP, UTP and ACh is achieved by release of Ca^{2+} from internal stores. Once ATP, UTP and ACh stimulate their corresponding receptors (P2Y and M3R), DAG and IP_3 are produced through PLC. DAG activates PKC family members and IP_3 binds to its receptor on the endoplasmic reticulum, which eventually cause the release of Ca^{2+} from internal stores (Bordin et al., 1995; MacDonald et al., 2005; Azua et al., 2011). Our data of showing increased insulin secretion by receptor stimulation in Min6 (Fig. 3.6) was in line with studies by the groups of Gilon and Henquin, (2001); Nesher et al., (2002); Tengholm and Gylfe, (2009); Balasubramanian et al., (2010), in which insulin secretion was stimulated by ATP, UTP and ACh. When rapamycin was added alongside the receptor stimulators, insulin

secretion was not increased above basal levels of secretion (Fig. 3.8).
Since the activation of P2Y and M3R receptors leads to the release of Ca^{2+} from internal store, we assessed the changes in $[Ca^{2+}]i$ during treatment of the cells with ATP, UTP and ACh in the presence and absence of rapamycin using FlexStation 3 (see Section 4.6 below).

4.5 The effect of rapamycin treatment on Min6 cells was not reversible after 6 hours of recovery

Although different groups have investigated the effects of different agonists on insulin secretion (Gilon and Henquin, 2001; Nesher et al., 2002; Tengholm and Gylfe, 2009), exposure of cells or islets to rapamycin for a short time (1 hour) followed by recovery period (1 hour or 6 hours) with regards to GSIS has not been previously assessed. Our work indicates that the rapamycin effect on insulin secretion was not reversible after 6 hours of recovery time in normal culture medium (Fig.3.10, 3.11 and 3.12).

According to published data, when glucose responsive Min6 cells are stimulated with high glucose concentration (up to 25 mM), glucose is transported into the cells via Glut-2 and metabolized. The subsequent elevation in ATP/ADP ratio leads to closure of the K_{ATP} channels. This event would cause membrane depolarization that leads to the opening of the voltage-dependent Ca^{2+} channels and increased $[Ca^{2+}]_i$, followed by insulin exocytosis (Cheng et al., 2012). The increase in ATP level is also required for insulin granule maturation and trafficking from the reserve pool to cell surface (Hou et al., 2009). Hence it can be seen that ATP generation plays an important role in glucose-induced insulin secretion. The groups of Barlow et al., (2013); Groenewoud and Zwartkruis, (2013); Morita et al., (2013) reported that rapamycin has a direct impact on glycolysis, mitochondrial function and ATP production. Hence, when treating the cells with rapamycin, the drug may interfere with ATP production, increases in $[Ca^{2+}]_i$ and insulin granule trafficking.

Therefore, we wanted to assess the changes in ATP level by using CellTiter-Glo luminescent cell viability assay by Promega. No significant changes in ATP levels were observed in our study (Fig. 3.13). However, this experiment was attempted only once (n=1) with no positive control. Therefore, further investigation is required to evaluate the effect of rapamycin on ATP production using this assay, or an alternative

method for testing ATP levels to confirm the results of Barlow et al (2013) and others.

4.6 Rapamycin had no effect on intracellular Ca^{2+} levels when purinergic and muscarinic receptors were activated by ATP + UTP and ACh

We know that ATP, UTP and ACh lead to increase in intracellular Ca^{2+} concentrations ($[Ca^{2+}]_i$) from internal stores through DAG, IP_3 and PKC. In the current study, we demonstrated that rapamycin reduced insulin secretion resulting from β-cell receptor activation by ATP, UTP and ACh. We therefore wanted to test if rapamycin would have an effect on $[Ca^{2+}]_i$ using the FlexStation 3 after stimulating the cells with high glucose (20 mM), ATP+UTP (100 μM), ACh (100 μM) or high KCl concentration (40 mM).

Although the Min6 cells used in these particular experiments did not show significant $[Ca^{2+}]_i$ changes with 20mM glucose, muscarinic (M3R) and purinergic receptor stimulation and chemical depolarization (using KCl) led to robust changes in $[Ca^{2+}]_i$ (Fig. 3.14 Panel A). As mentioned earlier, loss of glucose responsiveness in Min6 cells has been previously reported, and explained in (Miyazaki et al., 1990; Cheng et al., 2012; Kobayashi et al., 2016).

Interestingly, no significant change in peak $[Ca^{2+}]_i$ signal was observed when rapamycin was added to the ATP/UTP mix, as well as Ach treatment (Fig. 3.14 Panel B). Also, when the cells were depolarized with high concentration of KCl (40 mM), the Ca^{2+} signal was not significantly different when rapamycin was present.

These findings suggest that rapamycin had no effect on either voltage-dependent Ca^{2+} channels or the muscarinic and purinergic receptor stimulated signaling pathways. This means that rapamycin is likely to inhibit later events in insulin signaling such as recruitment of insulin granules from the reserve pool, granule movement, or granule docking at the cell membrane. Further studies are therefore required to fully elucidate the mechanism of rapamycin-induced inhibition of insulin secretion.

4.7 Conclusion

In this project we showed that rapamycin significantly reduced the rate of cell proliferation over a 4 day period of treatment, in agreement with published literature. Although we assessed cell death by trypan blue exclusion, and separately using a commercial caspase 3/7 activity assay, no increased cell death was observed. As this is contradictory to previously published data in Min6 cells, it is recommended that further investigation of cell death is made using alternative techniques such as TUNEL assays. We also showed that Min6 cells secreted insulin when stimulated with ATP, UTP and ACh, supporting published data. However, insulin secretion was prevented when rapamycin was present. Furthermore, preincubation with rapaycin for 30 minutes showed a long-lasting inhibitory effect, suggesting an irreversible mechanism of inhibition. Finally, rapamycin did not influence changes in intracellular $[Ca^{2+}]_i$ brought about by different stimulators of insulin release. This could mean that rapamycin might be involved in the inhibition of events later in insulin signaling such as recruitment of insulin granules from the reserve pool (Ca^{2+}-dependent), granule movement or docking with the cell membrane.

Effects on other aspects of β-cell physiology cannot be ruled out entirely (e.g. ATP generation following glucose stimulation, insulin biosynthesis), although evidence from these experiments suggests a fundamental step is inhibited in order to prevent insulin secretion via multiple different mechanisms (i.e. not just glucose metabolism). Therefore, further investigation is required to fully elucidate the mechanism of how rapamycin inhibits insulin secretion.

Chapter 5:

References

AITTONIEMI, J., FOTINOU, C., CRAIG, T. J., DE WET, H., PROKS, P. & ASHCROFT, F. M. 2009. SUR1: a unique ATP-binding cassette protein that functions as an ion channel regulator. *Philosophical Transactions of the Royal Society B: Biological Sciences,* 364**,** 257-267.

ARNOUX, J.-B., VERKARRE, V., SAINT-MARTIN, C., MONTRAVERS, F., BRASSIER, A., VALAYANNOPOULOS, V., BRUNELLE, F., FOURNET, J.-C., ROBERT, J.-J., AIGRAIN, Y., BELLANNÉ-CHANTELOT, C. & DE LONLAY, P. 2011. Congenital hyperinsulinism: current trends in diagnosis and therapy. *Orphanet Journal of Rare Diseases,* 6**,** 1-14.

BALASUBRAMANIAN, R., DE AZUA, I. R., WESS, J. & JACOBSON, K. A. 2010. Activation of distinct P2Y receptor subtypes stimulates insulin secretion in MIN6 mouse pancreatic β cells. *Biochemical pharmacology,* 79**,** 1317-1326.

BALLOU, L. M. & LIN, R. Z. 2008. Rapamycin and mTOR kinase inhibitors. *Journal of chemical biology,* 1**,** 27-36.

BARLOW, A., XIE, J., MOORE, C., CAMPBELL, S., SHAW, J., NICHOLSON, M. & HERBERT, T. 2012. Rapamycin toxicity in MIN6 cells and rat and human islets is mediated by the inhibition of mTOR complex 2 (mTORC2). *Diabetologia,* 55**,** 1355-1365.

BARLOW, A. D., NICHOLSON, M. L. & HERBERT, T. P. 2013. Evidence for rapamycin toxicity in pancreatic β-cells and a review of the underlying molecular mechanisms. *Diabetes,* 62**,** 2674-2682.

BELL, E., CAO, X., MOIBI, J. A., GREENE, S. R., YOUNG, R., TRUCCO, M., GAO, Z., MATSCHINSKY, F. M., DENG, S. & MARKMAN, J. F. 2003. Rapamycin has a deleterious effect on MIN-6 cells and rat and human islets. *Diabetes,* 52**,** 2731-2739.

BELLANNÉ-CHANTELOT, C., SAINT-MARTIN, C., RIBEIRO, M.-J., VAURY, C., VERKARRE, V., ARNOUX, J.-B., VALAYANNOPOULOS, V., GOBRECHT, S., SEMPOUX, C. & RAHIER, J. 2010. ABCC8 and KCNJ11 molecular spectrum of 109 patients with diazoxide-unresponsive congenital hyperinsulinism. *Journal of Medical Genetics,* 47**,** 752-759.

BERETTA, L., GINGRAS, A., SVITKIN, Y., HALL, M. & SONENBERG, N. 1996. Rapamycin blocks the phosphorylation of 4E-BP1 and inhibits cap-dependent initiation of translation. *The EMBO journal,* 15**,** 658.

BLANDINO-ROSANO, M., CHEN, A. Y., SCHEYS, J. O., ALEJANDRO, E. U., GOULD, A. P., TARANUKHA, T., ELGHAZI, L., CRAS-MÉNEUR, C. & BERNAL-MIZRACHI, E. 2012. mTORC1 signaling and regulation of pancreatic β-cell mass. *Cell Cycle,* 11**,** 1892-1902.

BORDIN, S., BOSCHERO, A., CARNEIRO, E. & ATWATER, I. 1995. Ionic mechanisms involved in the regulation of insulin secretion by muscarinic agonists. *The Journal of membrane biology,* 148**,** 177-184.

BOSCHERO, A., SZPAK-GLASMAN, M., CARNEIRO, E., BORDIN, S., PAUL, I., ROJAS, E. & ATWATER, I. 1995. Oxotremorine-m potentiation of glucose-induced insulin release from rat islets involves M3 muscarinic receptors. *American Journal of Physiology-Endocrinology and Metabolism,* 268**,** E336-E342.

BRONSTEIN-SITTON, N. 2006. Somatostatin and the somatostatin receptors: versatile regulators of biological activity. *Pathways,* 6.

BRUNI, A., GALA-LOPEZ, B., PEPPER, A. R., ABUALHASSAN, N. S. & SHAPIRO, A. 2014. Islet cell transplantation for the treatment of type 1 diabetes: recent advances and future challenges. *Diabetes Metab Syndr Obes,* 7**,** 211-223.

BURNSTOCK, G. & NOVAK, I. 2013. Purinergic signalling and diabetes. *Purinergic signalling,* 9**,** 307-324.

BUSSIERE, C., LAKEY, J., SHAPIRO, A. & KORBUTT, G. 2006. The impact of the mTOR inhibitor sirolimus on the proliferation and function of pancreatic islets and ductal cells. *Diabetologia,* 49**,** 2341-2349.

CAO, Z.-H., YIN, W.-D., ZHENG, Q.-Y., FENG, S.-L., XU, G.-L. & ZHANG, K.-Q. 2013. Caspase-3 is involved in IFN-γ-and TNF-α-Mediated MIN6 Cells Apoptosis via NF-κB/Bcl-2 Pathway. *Cell biochemistry and biophysics,* 67**,** 1239-1248.

CHANDRAN, S., PENG, F. Y. K., RAJADURAI, V. S., TE LU, Y., CHANG, K. T., FLANAGAN, S., ELLARD, S. & HUSSAIN, K. 2013. Paternally inherited ABCC8 mutation causing diffuse congenital hyperinsulinism. *Endocrinology, diabetes & metabolism case reports,* 2013.

CHENG, K., DELGHINGARO-AUGUSTO, V., NOLAN, C. J., TURNER, N., HALLAHAN, N., ANDRIKOPOULOS, S. & GUNTON, J. E. 2012. High

passage MIN6 cells have impaired insulin secretion with impaired glucose and lipid oxidation. *PloS one,* 7**,** e40868.

CHITNIS, M. M., YUEN, J. S., PROTHEROE, A. S., POLLAK, M. & MACAULAY, V. M. 2008. The type 1 insulin-like growth factor receptor pathway. *Clinical Cancer Research,* 14**,** 6364-6370.

D'AMICO, E., HUI, H., KHOURY, N., DI MARIO, U. & PERFETTI, R. 2005. Pancreatic β-cells expressing GLP-1 are resistant to the toxic effects of immunosuppressive drugs. *Journal of molecular endocrinology,* 34**,** 377-390.

DE LEÓN, D. D. & STANLEY, C. A. 2007. Mechanisms of disease: advances in diagnosis and treatment of hyperinsulinism in neonates. *Nature Clinical Practice Endocrinology & Metabolism,* 3**,** 57-68.

DE LONLAY-DEBENEY, P., POGGI-TRAVERT, F., FOURNET, J.-C., SEMPOUX, C., VICI, C. D., BRUNELLE, F., TOUATI, G., RAHIER, J., JUNIEN, C. & NIHOUL-FÉKÉTÉ, C. 1999. Clinical features of 52 neonates with hyperinsulinism. *New England Journal of Medicine,* 340**,** 1169-1175.

DEBERARDINIS, R. J., LUM, J. J., HATZIVASSILIOU, G. & THOMPSON, C. B. 2008. The biology of cancer: metabolic reprogramming fuels cell growth and proliferation. *Cell metabolism,* 7**,** 11-20.

DOYLE, M. E. & EGAN, J. M. 2003. Pharmacological agents that directly modulate insulin secretion. *Pharmacological Reviews,* 55**,** 105-131.

DUNNE, M. J., COSGROVE, K. E., SHEPHERD, R. M., AYNSLEY-GREEN, A. & LINDLEY, K. J. 2004. Hyperinsulinism in infancy: from basic science to clinical disease. *Physiological Reviews,* 84**,** 239-275.

ELMORE, S. 2007. Apoptosis: a review of programmed cell death. *Toxicologic pathology,* 35**,** 495-516.

ENKVETCHAKUL, D. & NICHOLS, C. G. 2003. Gating Mechanism of KATP Channels Function Fits Form. *The Journal of general physiology,* 122**,** 471-480.

FRAENKEL, M., KETZINEL-GILAD, M., ARIAV, Y., PAPPO, O., KARACA, M., CASTEL, J., BERTHAULT, M.-F., MAGNAN, C., CERASI, E. & KAISER, N. 2008. mTOR inhibition by rapamycin prevents β-cell adaptation to hyperglycemia and exacerbates the metabolic state in type 2 diabetes. *Diabetes,* 57**,** 945-957.

FUHRER, D., KOBAYASHI, M. & JIANG, H. 2001. Insulin release and suppression by tacrolimus, rapamycin and cyclosporin A are through regulation of the ATP-sensitive potassium channel. *Diabetes, Obesity and Metabolism,* 3**,** 393-402.

GAN, X., WANG, J., SU, B. & WU, D. 2011. Evidence for direct activation of mTORC2 kinase activity by phosphatidylinositol 3, 4, 5-trisphosphate. *Journal of Biological Chemistry,* 286**,** 10998-11002.

GILON, P. & HENQUIN, J.-C. 2001. Mechanisms and physiological significance of the cholinergic control of pancreatic β-cell function. *Endocrine reviews,* 22**,** 565-604.

GLASER, B. Hyperinsulinism of the newborn. Seminars in perinatology, 2000. Elsevier, 150-163.

GLATSTEIN, M., SCOLNIK, D. & BENTUR, Y. 2012. Octreotide for the treatment of sulfonylurea poisoning. *Clinical Toxicology,* 50**,** 795-804.

GLEASON, C. E., LU, D., WITTERS, L. A., NEWGARD, C. B. & BIRNBAUM, M. J. 2007. The role of AMPK and mTOR in nutrient sensing in pancreatic β-cells. *Journal of Biological Chemistry,* 282**,** 10341-10351.

GONZÁLEZ-BARROSO, M. M., GIURGEA, I., BOUILLAUD, F., ANEDDA, A., BELLANNÉ-CHANTELOT, C., HUBERT, L., DE KEYZER, Y., DE LONLAY, P. & RICQUIER, D. 2008. Mutations in UCP2 in congenital hyperinsulinism reveal a role for regulation of insulin secretion. *PloS one,* 3**,** e3850.

GRAVES, L. M., BORNFELDT, K. E., ARGAST, G. M., KREBS, E. G., KONG, X., LIN, T. A. & LAWRENCE, J. C. 1995. cAMP-and rapamycin-sensitive regulation of the association of eukaryotic initiation factor 4E and the translational regulator PHAS-I in aortic smooth muscle cells. *Proceedings of the National Academy of Sciences,* 92**,** 7222-7226.

GROENEWOUD, M. J. & ZWARTKRUIS, F. J. 2013. Rheb and mammalian target of rapamycin in mitochondrial homoeostasis. *Open biology,* 3**,** 130185.

GÜEMES, M., RAHMAN, S. A. & HUSSAIN, K. 2016. What is a normal blood glucose? *Archives of Disease in Childhood,* 101**,** 569-574.

HALL, P. & LEVISON, D. 1990. Review: assessment of cell proliferation in histological material. *Journal of clinical pathology,* 43**,** 184.

HARA, K., MARUKI, Y., LONG, X., YOSHINO, K.-I., OSHIRO, N., HIDAYAT, S., TOKUNAGA, C., AVRUCH, J. & YONEZAWA, K. 2002. Raptor, a binding partner of target of rapamycin (TOR), mediates TOR action. *Cell,* 110**,** 177-189.

HATTORI, M. & GOUAUX, E. 2012. Molecular mechanism of ATP binding and ion channel activation in P2X receptors. *Nature,* 485**,** 207-212.

HAY, N. & SONENBERG, N. 2004. Upstream and downstream of mTOR. *Genes & development,* 18**,** 1926-1945.

HEMMINGS, B. A. & RESTUCCIA, D. F. 2012. Pi3k-pkb/akt pathway. *Cold Spring Harbor perspectives in biology,* 4**,** a011189.

HIDALGO, M. & ROWINSKY, E. K. 2000. The rapamycin-sensitive signal transduction pathway as a target for cancer therapy. *Oncogene,* 19.

HONG, S. Y., YU, F.-X., LUO, Y. & HAGEN, T. 2016. Oncogenic activation of the PI3K/Akt pathway promotes cellular glucose uptake by downregulating the expression of thioredoxin-interacting protein. *Cellular signalling,* 28**,** 377-383.

HOU, J. C., MIN, L. & PESSIN, J. E. 2009. Insulin granule biogenesis, trafficking and exocytosis. *Vitamins & Hormones,* 80**,** 473-506.

HUANG, T., LIN, X., MENG, X. & LIN, M. 2014. Phosphoinositide-3 kinase/protein kinase-B/mammalian target of rapamycin pathway in psoriasis pathogenesis. A potential therapeutic target? *Acta dermato-venereologica,* 94**,** 371-379.

HUSSAIN, K. 2007. Insights in congenital hyperinsulinism. *Congenital Endocrinopathies*. Karger Publishers.

ISHIHARA, H., ASANO, T., TSUKUDA, K., KATAGIRI, H., INUKAI, K., ANAI, M., KIKUCHI, M., YAZAKI, Y., MIYAZAKI, J.-I. & OKA, Y. 1993. Pancreatic beta cell line MIN6 exhibits characteristics of glucose metabolism and glucose-stimulated insulin secretion similar to those of normal islets. *Diabetologia,* 36**,** 1139-1145.

JAMES, C., KAPOOR, R. R., ISMAIL, D. & HUSSAIN, K. 2009. The genetic basis of congenital hyperinsulinism. *Journal of Medical Genetics,* 46**,** 289-299.

JEFFERIES, H., REINHARD, C., KOZMA, S. & THOMAS, G. 1994. Rapamycin selectively represses translation of the" polypyrimidine tract" mRNA family. *Proceedings of the National Academy of Sciences,* 91**,** 4441-4445.

JOHNSON, D., SHEPHERD, R. M., GILL, D., GORMAN, T., SMITH, D. M. & DUNNE, M. J. 2007. Glucose-dependent modulation of insulin secretion and

intracellular calcium ions by GKA50, a glucokinase activator. *Diabetes,* 56**,** 1694-1702.

JÓZWIAK, P., FORMA, E., BRYS, M. & KRZESLAK, A. 2015. O-GlcNAcylation and metabolic reprograming in cancer. *30 years old: O-GlcNAc reaches age of reason-Regulation of cell signaling and metabolism by O-GlcNAcylation***,** 62.

KATSNELSON, A. 2010. Biologists tackle cells' identity crisis. *Nature,* 465**,** 537-537.

KHAN, S., YAN-DO, R., DUONG, E., WU, X., BAUTISTA, A., CHELEY, S., MACDONALD, P. E. & BRAUN, M. 2014. Autocrine activation of P2Y1 receptors couples Ca2+ influx to Ca2+ release in human pancreatic beta cells. *Diabetologia,* 57**,** 2535-2545.

KLOSTER-JENSEN, K., SAHRAOUI, A., VETHE, N. T., KORSGREN, O., BERGAN, S., FOSS, A. & SCHOLZ, H. 2016. Treatment with Tacrolimus and Sirolimus Reveals No Additional Adverse Effects on Human Islets In Vitro Compared to Each Drug Alone but They Are Reduced by Adding Glucocorticoids. *Journal of diabetes research,* 2016.

KOBAYASHI, M., YAMATO, E., TANABE, K., TASHIRO, F., MIYAZAKI, S. & MIYAZAKI, J.-I. 2016. Functional Analysis of Novel Candidate Regulators of Insulin Secretion in the MIN6 Mouse Pancreatic β Cell Line. *PloS one,* 11**,** e0151927.

LAPLANTE, M. & SABATINI, D. M. 2009. mTOR signaling at a glance. *Journal of cell science,* 122**,** 3589-3594.

LE BACQUER, O., QUENIAT, G., GMYR, V., KERR-CONTE, J., LEFEBVRE, B. & PATTOU, F. 2013. mTORC1 and mTORC2 regulate insulin secretion through Akt in INS-1 cells. *Journal of Endocrinology,* 216**,** 21-29.

LENZEN, S. 2014. A fresh view of glycolysis and glucokinase regulation: history and current status. *Journal of Biological Chemistry,* 289**,** 12189-12194.

LI, Y., CAO, X., LI, L.-X., BRUBAKER, P. L., EDLUND, H. & DRUCKER, D. J. 2005. β-Cell Pdx1 expression is essential for the glucoregulatory, proliferative, and cytoprotective actions of glucagon-like peptide-1. *Diabetes,* 54**,** 482-491.

MACDONALD, P. E., JOSEPH, J. W. & RORSMAN, P. 2005. Glucose-sensing mechanisms in pancreatic β-cells. *Philosophical Transactions of the Royal Society of London B: Biological Sciences,* 360**,** 2211-2225.

MINAMI, K., YANO, H., MIKI, T., NAGASHIMA, K., WANG, C.-Z., TANAKA, H., MIYAZAKI, J.-I. & SEINO, S. 2000. Insulin secretion and differential gene expression in glucose-responsive and-unresponsive MIN6 sublines. *American Journal of Physiology-Endocrinology and Metabolism,* 279**,** E773-E781.

MIYAZAKI, J.-I., ARAKI, K., YAMATO, E., IKEGAMI, H., ASANO, T., SHIBASAKI, Y., OKA, Y. & YAMAMURA, K.-I. 1990. Establishment of a Pancreatic β Cell Line That Retains Glucose-Inducible Insulin Secretion: Special Reference to Expression of Glucose Transporter Isoforms*. *Endocrinology,* 127**,** 126-132.

MORITA, M., GRAVEL, S.-P., CHÉNARD, V., SIKSTRÖM, K., ZHENG, L., ALAIN, T., GANDIN, V., AVIZONIS, D., ARGUELLO, M. & ZAKARIA, C. 2013. mTORC1 controls mitochondrial activity and biogenesis through 4E-BP-dependent translational regulation. *Cell metabolism,* 18**,** 698-711.

NESHER, R., ANTEBY, E., YEDOVIZKY, M., WARWAR, N., KAISER, N. & CERASI, E. 2002. β-Cell protein kinases and the dynamics of the insulin response to glucose. *Diabetes,* 51**,** S68-S73.

NESTOROWICZ, A., WILSON, B. A., SCHOOR, K. P., INOUE, H., GLASER, B., LANDAU, H., STANLEY, C. A., THORNTON, P. S., CLEMENT, J. P. & BRYAN, J. 1996. Mutations in the sulfonylurea receptor gene are associated with familial hyperinsulinism in Ashkenazi Jews. *Human molecular genetics,* 5**,** 1813-1822.

NICLAUSS, N., BOSCO, D., MOREL, P., GIOVANNONI, L., BERNEY, T. & PARNAUD, G. 2011. Rapamycin impairs proliferation of transplanted islet β cells. *Transplantation,* 91**,** 714-722.

ORGANISATION, W. H. 1999. *WHO laboratory manual for the examination of human semen and sperm-cervical mucus interaction*, Cambridge university press.

PETERSON, T. R., LAPLANTE, M., THOREEN, C. C., SANCAK, Y., KANG, S. A., KUEHL, W. M., GRAY, N. S. & SABATINI, D. M. 2009. DEPTOR is an mTOR inhibitor frequently overexpressed in multiple myeloma cells and required for their survival. *Cell,* 137**,** 873-886.

PETIT, P., BERTRAND, G., SCHMEER, W. & HENQUIN, J.-C. 1989. Effects of extracellular adenine nucleotides on the electrical, ionic and secretory events in mouse pancreatic β-cells. *British journal of pharmacology,* 98**,** 875-882.

PÓPULO, H., LOPES, J. M. & SOARES, P. 2012. The mTOR signalling pathway in human cancer. *International journal of molecular sciences,* 13**,** 1886-1918.

POULSEN, C. R., BOKVIST, K., OLSEN, H. L., HØY, M., CAPITO, K., GILON, P. & GROMADA, J. 1999. Multiple sites of purinergic control of insulin secretion in mouse pancreatic beta-cells. *Diabetes,* 48**,** 2171-2181.

PRIESTLEY, A., BEAMISH, H., SINGLETON, B., BLUNT, T., JEGGO, P., GELL, D., SMITH, G., JACKSON, S., AMATUCCI, A. & TACCIOLI, G. 1998. Molecular and biochemical characterisation of DNA-dependent protein kinase-defective rodent mutant irs-20. *Nucleic acids research,* 26**,** 1965-1973.

RAHIER, J., GUIOT, Y. & SEMPOUX, C. 2000. Persistent hyperinsulinaemic hypoglycaemia of infancy: a heterogeneous syndrome unrelated to nesidioblastosis. *Archives of Disease in Childhood-Fetal and Neonatal Edition,* 82**,** F108-F112.

REUBI, J., SCHAER, J., MARKWALDER, R., WASER, B., HORISBERGER, U. & LAISSUE, J. 1997. Distribution of somatostatin receptors in normal and neoplastic human tissues: recent advances and potential relevance. *The Yale journal of biology and medicine,* 70**,** 471.

RICHARDS-WILLIAMS, C., CONTRERAS, J. L., BERECEK, K. H. & SCHWIEBERT, E. M. 2008. Extracellular ATP and zinc are co-secreted with insulin and activate multiple P2X purinergic receptor channels expressed by islet beta-cells to potentiate insulin secretion. *Purinergic signalling,* 4**,** 393-405.

ROTHENBERG, P. L., WILLISON, L. D. & WOLF, B. A. 1995. Glucose-induced insulin receptor tyrosine phosphorylation in insulin-secreting β-cells. *Diabetes,* 44**,** 802-809.

SARBASSOV, D. D., ALI, S. M., SENGUPTA, S., SHEEN, J.-H., HSU, P. P., BAGLEY, A. F., MARKHARD, A. L. & SABATINI, D. M. 2006. Prolonged rapamycin treatment inhibits mTORC2 assembly and Akt/PKB. *Molecular cell,* 22**,** 159-168.

SCHREIBER, K. H., ORTIZ, D., ACADEMIA, E. C., ANIES, A. C., LIAO, C. Y. & KENNEDY, B. K. 2015. Rapamycin-mediated mTORC2 inhibition is

determined by the relative expression of FK506-binding proteins. *Aging cell,* 14**,** 265-273.

SCHWIEBERT, E. M., LIANG, L., CHENG, N.-L., WILLIAMS, C. R., OLTEANU, D., WELTY, E. A. & ZSEMBERY, A. 2005. Extracellular zinc and ATP-gated P2X receptor calcium entry channels: New zinc receptors as physiological sensors and therapeutic targets. *Purinergic signalling,* 1**,** 299-310.

SCHWIEBERT, E. M. & ZSEMBERY, A. 2003. Extracellular ATP as a signaling molecule for epithelial cells. *Biochimica et Biophysica Acta (BBA)-Biomembranes,* 1615**,** 7-32.

SEHGAL, S. Sirolimus: its discovery, biological properties, and mechanism of action. Transplantation proceedings, 2003. Elsevier, S7-S14.

SEKULIĆ, A., HUDSON, C. C., HOMME, J. L., YIN, P., OTTERNESS, D. M., KARNITZ, L. M. & ABRAHAM, R. T. 2000. A direct linkage between the phosphoinositide 3-kinase-AKT signaling pathway and the mammalian target of rapamycin in mitogen-stimulated and transformed cells. *Cancer research,* 60**,** 3504-3513.

SEMPOUX, C., GUIOT, Y., JAUBERT, F. & RAHIER, J. 2004. Focal and diffuse forms of congenital hyperinsulinism: the keys for differential diagnosis. *Endocrine pathology,* 15**,** 241-246.

SENNIAPPAN, S., ARYA, V. B. & HUSSAIN, K. 2013a. The molecular mechanisms, diagnosis and management of congenital hyperinsulinism. *Indian journal of endocrinology and metabolism,* 17**,** 19.

SENNIAPPAN, S., BROWN, R. E. & HUSSAIN, K. 2016. Genomic and morphoproteomic correlates implicate the IGF-1/mTOR/Akt pathway in the pathogenesis of diffuse congenital hyperinsulinism. *INTERNATIONAL JOURNAL OF CLINICAL AND EXPERIMENTAL PATHOLOGY,* 9**,** 548-562.

SENNIAPPAN, S., HINDMARSH, P. & HUSSAIN, K. 2013b. Gene expression profiling reveals possible role of growth factors in beta cell hyperplasia in congenital hyperinsulinism.

SHAH, P., ARYA, V. B., FLANAGAN, S. E., MORGAN, K., ELLARD, S., SENNIAPPAN, S. & HUSSAIN, K. 2015. Sirolimus therapy in a patient with severe hyperinsulinaemic hypoglycaemia due to a compound heterozygous

ABCC8 gene mutation. *Journal of Pediatric Endocrinology and Metabolism,* 28**,** 695-699.

SHIMOBAYASHI, M. & HALL, M. N. 2014. Making new contacts: the mTOR network in metabolism and signalling crosstalk. *Nature reviews Molecular cell biology,* 15**,** 155-162.

SKELIN, M., RUPNIK, M. & CENCIC, A. 2010. Pancreatic beta cell lines and their applications in diabetes mellitus research. *Altex,* 27**,** 105-113.

STEWART, A. F., HUSSAIN, M. A., GARCÍA-OCAÑA, A., VASAVADA, R. C., BHUSHAN, A., BERNAL-MIZRACHI, E. & KULKARNI, R. N. 2015. Human β-cell proliferation and intracellular signaling: part 3. *Diabetes,* 64**,** 1872-1885.

SUN, C.-L., HAM, D.-S., PARK, H.-S., KIM, J.-W., CHO, J.-H., SONG, K.-H., SON, H.-Y. & YOON, K.-H. 2010. Rapamycin suppresses the expansion and differentiation of porcine neonatal pancreas cell clusters. *Transplantation,* 90**,** 717-724.

SZABAT, M., LYNN, F. C., HOFFMAN, B. G., KIEFFER, T. J., ALLAN, D. W. & JOHNSON, J. D. 2012. Maintenance of β-Cell Maturity and Plasticity in the Adult Pancreas Developmental Biology Concepts in Adult Physiology. *Diabetes,* 61**,** 1365-1371.

TENGHOLM, A. & GYLFE, E. 2009. Oscillatory control of insulin secretion. *Molecular and cellular endocrinology,* 297**,** 58-72.

THOMAS, P. M., WOHLLK, N., HUANG, E., KUHNLE, U., RABL, W., GAGEL, R. F. & COTE, G. J. 1996. Inactivation of the first nucleotide-binding fold of the sulfonylurea receptor, and familial persistent hyperinsulinemic hypoglycemia of infancy. *American journal of human genetics,* 59**,** 510.

TWIDDY, D., COHEN, G. M., MACFARLANE, M. & CAIN, K. 2006. Caspase-7 is directly activated by the~ 700-kDa apoptosome complex and is released as a stable XIAP-caspase-7~ 200-kDa complex. *Journal of Biological Chemistry,* 281**,** 3876-3888.

VEDOVATO, N., ASHCROFT, F. M. & PULJUNG, M. C. 2015. The Nucleotide-Binding Sites of SUR1: A Mechanistic Model. *Biophysical journal,* 109**,** 2452-2460.

WARD, P. S. & THOMPSON, C. B. 2012. Signaling in control of cell growth and metabolism. *Cold Spring Harbor perspectives in biology,* 4**,** a006783.

WUTTKE, A., IDEVALL-HAGREN, O. & TENGHOLM, A. 2013. P2Y1 receptor-dependent diacylglycerol signaling microdomains in β cells promote insulin secretion. *The FASEB Journal,* 27**,** 1610-1620.

YEN, C.-F., HUANG, C.-Y., CHAN, C.-I., HSU, C.-H., WANG, N.-L., WANG, T.-Y., LIN, C.-L. & TING, W.-H. 2016. Successful treatment of a newborn with congenital hyperinsulinism having a novel heterozygous mutation in the ABCC8 gene using subtotal pancreatectomy. *Tzu Chi Medical Journal*.

ZAHR, E., MOLANO, R., PILEGGI, A., ICHII, H., SAN JOSE, S., BOCCA, N., AN, W., GONZALEZ-QUINTANA, J., FRAKER, C. & RICORDI, C. Rapamycin impairs β-cell proliferation in vivo. Transplantation proceedings, 2008. Elsevier, 436-437.

ZENG, Z., SARBASSOV, D. D., SAMUDIO, I. J., YEE, K. W., MUNSELL, M. F., JACKSON, C. E., GILES, F. J., SABATINI, D. M., ANDREEFF, M. & KONOPLEVA, M. 2007. Rapamycin derivatives reduce mTORC2 signaling and inhibit AKT activation in AML. *Blood,* 109**,** 3509-3512.